Cell Reports

Article

The essential malaria protein *Pf*CyRPA targets glycans to invade erythrocytes

Graphical abstract

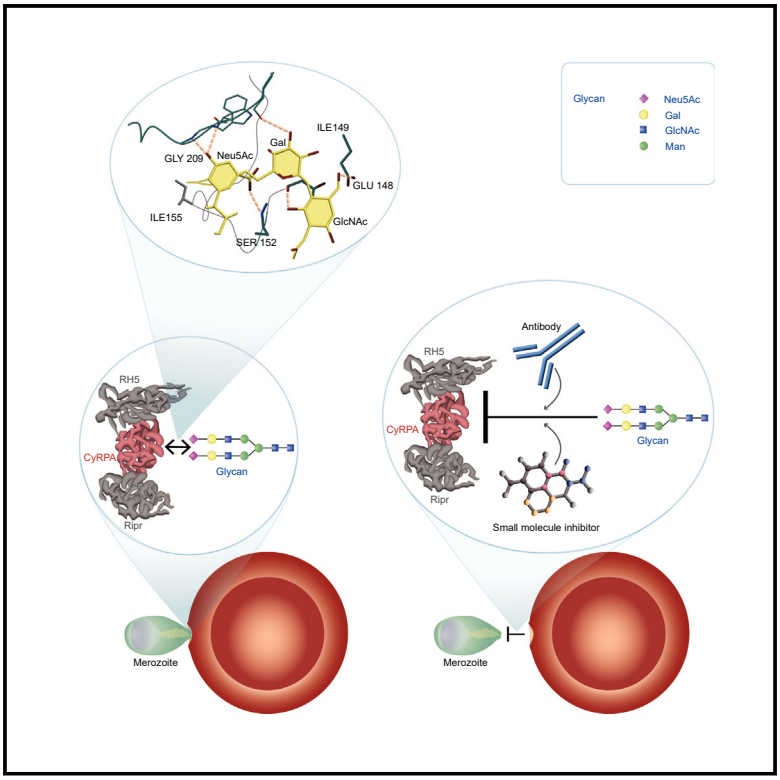

Highlights

- *Plasmodium falciparum* CyRPA binds to carbohydrates with terminal 2-6-linked Neu5Ac
- Lectin activity of *Plasmodium falciparum* CyRPA contributes to erythrocyte invasion
- Targeting lectin activity with drugs and antibodies is a promising anti-malarial strategy

Authors

Christopher J. Day, Paola Favuzza, Sabrina Bielfeld, ..., Michael Filarsky, Michael P. Jennings, Gerd Pluschke

Correspondence

m.jennings@griffith.edu.au (M.P.J.), gerd.pluschke@swisstph.ch (G.P.)

In brief

Day et al. show that the essential *Plasmodium falciparum* invasion protein PfCyRPA is a lectin targeting 2-6-linked Neu5Ac. Molecular modeling, mutagenesis, and transgenic parasite studies show that PfCyRPA lectin activity is required for erythrocyte invasion. Drug and antibody inhibitors validate this activity as a therapeutic target to prevent and treat malaria.

Day et al., 2024, Cell Reports *43*, 114012
April 23, 2024
https://doi.org/10.1016/j.celrep.2024.114012

CellPress

Cell Reports

CellPress
OPEN ACCESS

Article

The essential malaria protein *Pf*CyRPA targets glycans to invade erythrocytes

Christopher J. Day,[1,9] Paola Favuzza,[2,3,8,9] Sabrina Bielfeld,[4,5] Thomas Haselhorst,[1] Leonie Seefeldt,[2,3] Julia Hauser,[2,3] Lucy K. Shewell,[1] Christian Flueck,[2,3] Jessica Poole,[1] Freda E.-C. Jen,[1] Anja Schäfer,[2,3] Jean-Pierre Dangy,[2,3] Tim-W. Gilberger,[4,5,6] Camila Tenorio França,[7] Manoj T. Duraisingh,[7] Marco Tamborrini,[2,3] Nicolas M.B. Brancucci,[2,3] Christof Grüring,[2,3] Michael Filarsky,[4,5] Michael P. Jennings,[1,*] and Gerd Pluschke[2,3,10,*]

[1]Institute for Glycomics, Griffith University, Gold Coast, QLD, Australia
[2]Swiss Tropical and Public Health Institute, Allschwil, Switzerland
[3]University of Basel, Basel, Switzerland
[4]Centre for Structural Systems Biology (CSSB), Hamburg, Germany
[5]Department of Biology, University of Hamburg, Hamburg, Germany
[6]Department of Cellular Parasitology, Bernhard Nocht Institute for Tropical Medicine, Hamburg, Germany
[7]Department of Immunology & Infectious Diseases, Harvard TH Chan School of Public Health, Boston, MA, USA
[8]Present address: The Walter and Eliza Hall Institute of Medical Research, Parkville, VIC, Australia
[9]These authors contributed equally
[10]Lead contact
*Correspondence: m.jennings@griffith.edu.au (M.P.J.), gerd.pluschke@swisstph.ch (G.P.)
https://doi.org/10.1016/j.celrep.2024.114012

SUMMARY

Plasmodium falciparum is a human-adapted apicomplexan parasite that causes the most dangerous form of malaria. *P. falciparum* cysteine-rich protective antigen (*Pf*CyRPA) is an invasion complex protein essential for erythrocyte invasion. The precise role of *Pf*CyRPA in this process has not been resolved. Here, we show that *Pf*CyRPA is a lectin targeting glycans terminating with α2-6-linked N-acetylneuraminic acid (Neu5Ac). *Pf*CyRPA has a >50-fold binding preference for human, α2-6-linked Neu5Ac over non-human, α2-6-linked N-glycolylneuraminic acid. *Pf*CyRPA lectin sites were predicted by molecular modeling and validated by mutagenesis studies. Transgenic parasite lines expressing endogenous *Pf*CyRPA with single amino acid exchange mutants indicated that the lectin activity of *Pf*CyRPA has an important role in parasite invasion. Blocking *Pf*CyRPA lectin activity with small molecules or with lectin-site-specific monoclonal antibodies can inhibit blood-stage parasite multiplication. Therefore, targeting *Pf*CyRPA lectin activity with drugs, immunotherapy, or a vaccine-primed immune response is a promising strategy to prevent and treat malaria.

INTRODUCTION

Invasion of human erythrocytes by *Plasmodium falciparum* merozoites involves a complex cascade of highly specific molecular interactions between merozoite adhesins and host receptors mediating recognition, attachment, and active entry of the parasites into erythrocytes. Prior to tight junction formation, host cell "sensing" is mediated by the *P. falciparum* erythrocyte binding-like (*Pf*EBL) and reticulocyte binding protein homolog (*Pf*Rh) protein families.[1] With only one exception, i.e., *Pf*Rh5,[2] individual disruption of the *Pf*Rh- and *Pf*EBL-encoding genes does not prevent invasion, reflecting functional redundancy of the early receptor-ligand interactions.[3,4] Together with *P. falciparum* cysteine-rich protective antigen (*Pf*CyRPA)[5] and *P. falciparum* Rh5 interacting protein (*Pf*Ripr),[6] *Pf*Rh5 is part of a ternary invasion complex,[7] with all three components being refractory to genetic disruption and therefore essential.[2,6,8] Antibodies specific for each of the three components efficiently block parasite growth in both *in vitro* and *in vivo* models[5,6,9–12]; however, the mechanism by which invasion-blocking, anti-*Pf*CyRPA antibodies act is uncertain.[13]

RESULTS AND DISCUSSION

*Pf*CyRPA is a human sialic-acid-specific glycan-binding protein (lectin)

While basigin and SEMA7A function as erythrocyte receptors of *Pf*Rh5 and *Pf*Ripr, respectively,[14,15] the precise and essential role played by *Pf*CyRPA in the ternary *Pf*RH5-CyRPA-Ripr invasion complex is not clear. A recent structural analysis of the invasion complex concluded that "there is no known erythrocyte-binding partner for *Pf*CyRPA."[13] The 3D X-ray crystal structure of *Pf*CyRPA[11,16] revealed that it adopts a six-bladed β-propeller fold and that its overall structure resembles the catalytic domain of sialidases (α-linked sialic acid hydrolases). While *Pf*CyRPA contains an Asp box as its sialidase signature motif,[5] it lacks key residues necessary for catalysis, providing a structural correlate of the absence of sialidase activity.[11]

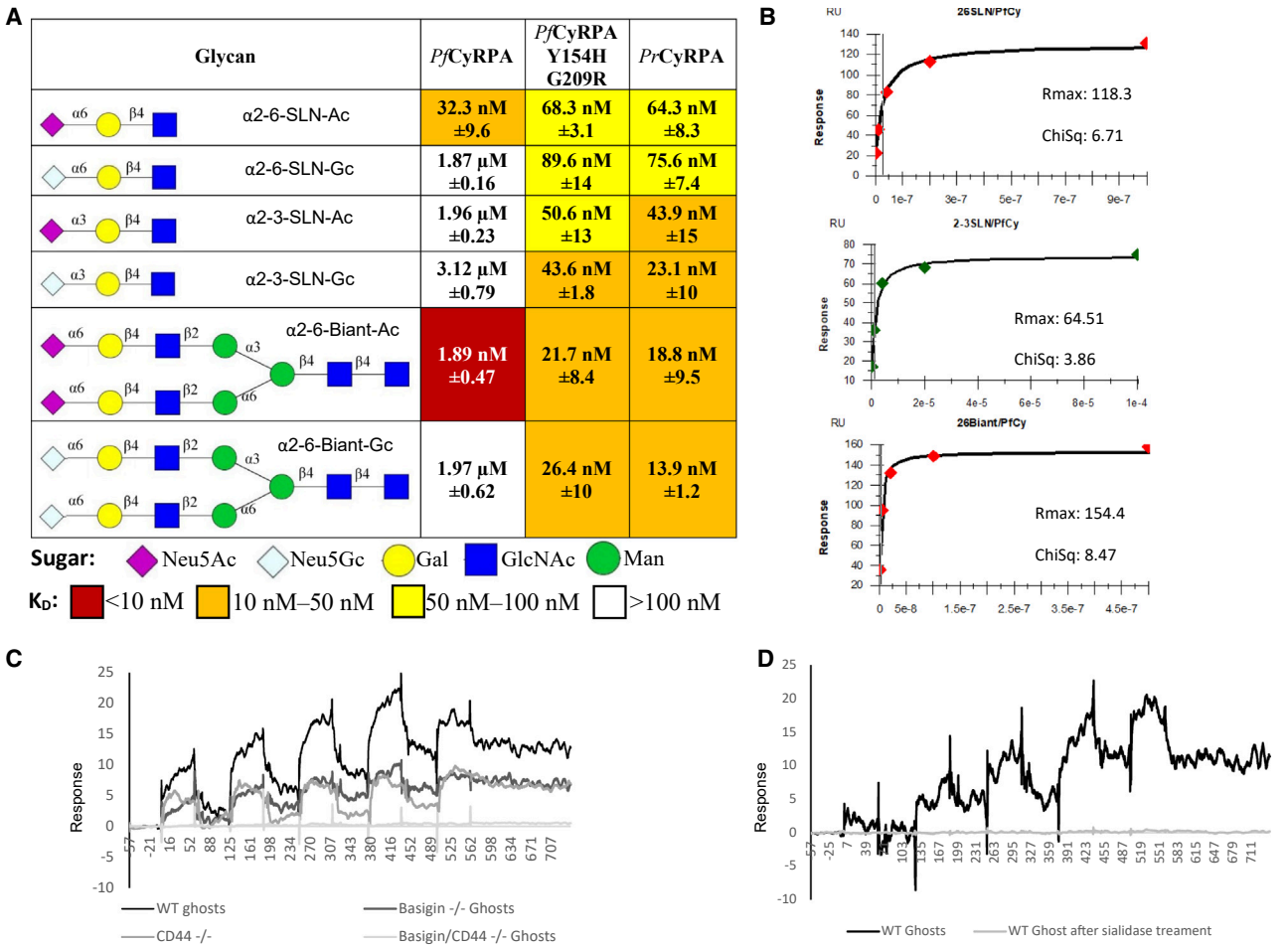

Figure 1. SPR analysis of glycan binding of CyRPA to synthetic glycans and erythrocyte ghosts

(A) Equilibrium dissociation constants (K_D) of glycan binding to CyRPA from *P. falciparum* (*Pf*) and *P. reichenowi* (*Pr*) and to a *Pf*CyRPA$_{Y154H/G209R}$ double mutant. Results of the glycan array experiments are the combination of three replicates. SPR assay data are an average of at least three replicate experiments shown as average ± standard deviation.

(B) Fit curves of *Pf*CyRPA with α2-6-SLN-Ac, α2-3-SLN-Ac, and α2-6-Biant-Ac.

(C) SPR analysis of *Pf*CyRPA binding to erythrocyte membranes. Lack of expression of basigin and/or CD44 was demonstrated by flow cytometric analysis (Figure S1).

(D) SPR analysis of *Pf*CyRPA binding to sialidase-treated erythrocyte membranes. SPR sensorgrams are shown in Figure S8.

Studies with recombinant proteins have demonstrated that the *Pf*Rh5-*Pf*CyRPA-*Pf*Ripr complex binds to erythroid cells with higher efficacy than *Pf*RH5 alone,[8] indicating a distinct role for *Pf*CyRPA in erythrocyte engagement. We hypothesized that *Pf*CyRPA evolved from a functional sialidase and lost its enzymatic activity, but retained sialic acid lectin activity to meet other functionalities. To test this hypothesis, we conducted a glycan microarray-based binding analysis to characterize *Pf*CyRPA lectin activity. Recombinantly expressed *Pf*CyRPA bound to 43/402 glycans present on a comprehensive glycan microarray[17] representing most major carbohydrate structures found in mammalian systems. The binding pattern indicated a preference for binding to glycans with sialic acid (Table S1). Quantitative surface plasmon resonance (SPR) analysis of binding kinetics identified a strong preference of *Pf*CyRPA for glycans terminating with α2-6-linked sialic acid (Neu5Ac [N-acetylneuraminic acid]). Furthermore, the trisaccharide, α2-6-N-acetylneuraminosyl lactosamine (Neu5Ac-α-(2-6)-Gal-β-(1-4)-GlcNAc), hereafter α2-6-SLN-Ac, which contains α2-6-linked Neu5Ac as the terminal motif, was identified as the highest-affinity monovalent candidate receptor (Figures 1A and 1B; Table S2). SPR analyses demonstrated a >50-fold preference of *Pf*CyRPA for α2-6-SLN-Ac over α2-3-SLN-Ac (disassociation constant [K_D] = 32.3 nM vs. 1.96 µM, respectively) (Figures 1A and 1B). A comparison of the structural models for α2-3-SLN-Ac and α2-6-SLN-Ac in complex with *Pf*CyRPA (Figures S2A and S2B, respectively) suggests that while the Neu5Ac moieties of α2-3-SLN-Ac and α2-6-SLN-Ac are bound in a similar conformation, the lactosamine core adopts a significantly different geometry, which is reflected by the nearly 40-fold higher binding affinity of α2-6-SLN-Ac compared to α2-3-SLN-Ac (32.3 nM vs. 1.96 µM; Figure 1A). Overall, the higher flexibility of the

α2-6-linkage between Neu5Ac and lactosamine likely enables α2-6-SLN-Ac to adopt a more "compact" conformation that can be compared with the characteristic "umbrella-like" structural topology that has been reported to be critical for efficient human adaptation and human-to-human transmission of influenza A viruses.[18]

The OK blood group antigen basigin has been identified as an erythrocytic target of the *Pf*Rh5 component of the *P. falciparum* invasion complex.[14] Basigin is closely associated on the erythrocyte surface with CD44 and glycophorin A.[19,20] All three proteins are known to be decorated with α2-6-linked Neu5Ac either as O-linked glycans (glycophorin A)[21] or complex biantennary N-linked glycans (basigin and CD44),[22] suggesting that carbohydrates associated with these proteins are candidate receptors for *Pf*CyRPA lectin activity. *Pf*CyRPA showed a more than 15-fold higher affinity to a commercially available biantennary glycan with α2-6-linked Neu5Ac terminal sialic acid (α2-6-Biant-Ac; K_D = 1.89 nM) than to the monomeric α2-6-SLN-Ac counterpart (32,3 nM; Figures 1A and 1B). This suggests that the N-linked biantennary glycans on basigin and CD44 are more likely to be targets than the O-linked glycans on glycophorin A. Consistent with this hypothesis, SPR studies showed that *Pf*CyRPA does not bind to immobilized membranes derived from immortalized erythroid cell lines lacking both basigin and CD44 (Figure 1C). Membranes from single basigin or CD44 knockout mutants showed reduced binding (Figure 1C). Similarly, removal of all sialic acid by sialidase treatment ablated *Pf*CyRPA binding to wild-type erythrocyte membranes (Figure 1D). We conclude that *Pf*CyRPA-mediated binding of merozoites to human erythrocytes is sialic-acid dependent and that α2-6-linked Neu5Ac N-linked biantennary glycans are likely targets.

*Pf*CyRPA has two lectin sites

We investigated the structural basis of *Pf*CyRPA α2-6-Neu5Ac lectin activity by molecular modeling and validated the results experimentally by *Pf*CyRPA mutagenesis studies (Figure 2). Molecular dynamics identified two sialic acid binding sites using unbiased docking; Neu5Ac site 1 (Figure 2A) was identified as being adjacent to the *Pf*CyRPA invasion-blocking monoclonal antibody (mAb) C12 epitope,[11] as depicted in the *Pf*CyRPA mAb C12 co-crystal structure (Figures 2A–2C). When α2-6-SLN-Ac was docked into a box placed at Neu5Ac binding site 1, *Pf*CyRPA residues belonging to blades 2 and 3 (E148, I149, S152, I155, and G209) were predicted to be involved in the major binding interactions within the α2-6-SLN-Ac-*Pf*CyRPA complex (Figure 2C). Glycan-binding studies with recombinantly expressed *Pf*CyRPA single-alanine exchange mutants validated the modeling predictions that identified lectin site 1 (Figures 2A–2C). The *Pf*CyRPA E148A mutant showed no α2-6-SLN-Ac binding, while the I149A, S152A, and I155A mutants showed reduced binding to α2-6-SLN-Ac, with 10- to 1,000-fold higher K_D values than wild-type *Pf*CyRPA (Figure 2D). Mutations at the 201-SHDKGETWG-209 loop had comparatively smaller effects (Figure 2D; Table S3). A detailed view of the interaction of *Pf*CyRPA residues E148, I149, S152, I155, and G-209 with α2-6-SLN-Ac is depicted in Figure 2C.

*Pf*CyRPA alanine exchange mutations also supported the modeling of Neu5Ac binding site 2, as the K_D of α2-6-Biant-Ac for the T100A and H134A *Pf*CyRPA site mutants was comparable with that of monovalent α2-6-SLN-Ac (>30 nM compared with 1.89 nM for wild-type *Pf*CyRPA; Figure 2D). Furthermore, site 2 D98A and T132A mutations weakened the binding of the biantennary glycan substantially (Figure 2D). The glutamic acid residue at position 148 is part of both lectin sites, and the E148A mutant showed binding neither to α2-6-SLN-Ac nor to the α2-6-Biant-Ac glycan (Figure 2D).The E148A mutation also affected the binding of the strongly growth-inhibitory mAb C12 (Figure 2D; Table S3), which interacts with *Pf*CyRPA residues immediately adjacent to E-148 (Y-144, N-145, and N-146) via van der Waals interactions.[11]

The presence of two sialic-acid-binding sites correlates with the high affinity for α2-6-Biant-Ac, the biantennary presentation of α2-6-Neu5Ac (Figure 1). Neither of the *Pf*CyRPA Neu5Ac lectin sites overlap with the regions that interact with *Pf*Rh5 on blades 4 and 5 or the *Pf*Ripr binding domain on blade 6 (Figure 2B) and therefore remain available for interactions with erythrocyte host glycans.

*Pf*CyRPA is adapted to recognize the sialic acid expressed by human erythrocytes

During the evolution of the genus *Homo*, approximately 3.2 million years ago, an exon deletion event occurred in the gene encoding cytidine monophosphate Neu5Ac hydroxylase (CMAH), which converts Neu5Ac to N-glycolylneuraminic acid (Neu5Gc).[23] Sialoglycans of all humans therefore contain only Neu5Ac, while non-human great ape sialoglycans contain both Neu5Gc and Neu5Ac, with Neu5Gc representing approximately 75% of the sialic acid presented on the surface of chimpanzee erythrocytes.[24] As the CMAH loss-of-function mutation is recessive, its increased frequency within the early human lineage must have been mediated by the selection of homozygous carriers.[25] Along these lines, it has been hypothesized that the loss of Neu5Gc temporarily relieved early humans from malignant malaria[26] and that *P. falciparum* emerged from ape-specific *Plasmodium reichenowi* by selective evolution of EBA175, which was considered one of the most important merozoite proteins involved in the initial erythrocyte recognition phase.[1] Glycophorin A and O-linked glycans are known receptors of EBA175 and facilitate merozoite binding to erythrocytes.[27] Changing preferential binding of EBA175 from Neu5Gc in the ape-specific *P. reichenowi* toward Neu5Ac has been suggested to account for the human-specific pathogenicity of *P. falciparum*.[28] However, EBA175 has subsequently been shown to be non-essential for erythrocyte invasion by *P. falciparum*.[4]

Our studies with *Pf*CyRPA and *P. reichenowi* CyRPA (*Pr*CyRPA) (Figures 1 and 2D) indicate that this invasion complex protein, essential in *P. falciparum*, has changed sialic acid specificity during co-evolution with the human host. *Pf*CyRPA has ~50-fold stronger binding to α2-6-SLN-Ac than to non-human Neu5Gc-containing α2-6-SLN-Gc (K_D = 32.3 nM vs. 1.87 μM) and greater than 1,000-fold stronger binding to the corresponding biantennary presentation of α2-6-Neu5Ac (α2-6-Biant-Ac) relative to the equivalent Neu5Gc (α2-6-Biant-Gc) structure (K_D = 1.89 nM vs. 1.97 μM; Figure 1). By contrast, non-human great ape-adapted *Pr*CyRPA showed a preference for neither sialic acid linkage, i.e., α2-6-Neu5Ac vs. α2-3-Neu5Ac, nor for

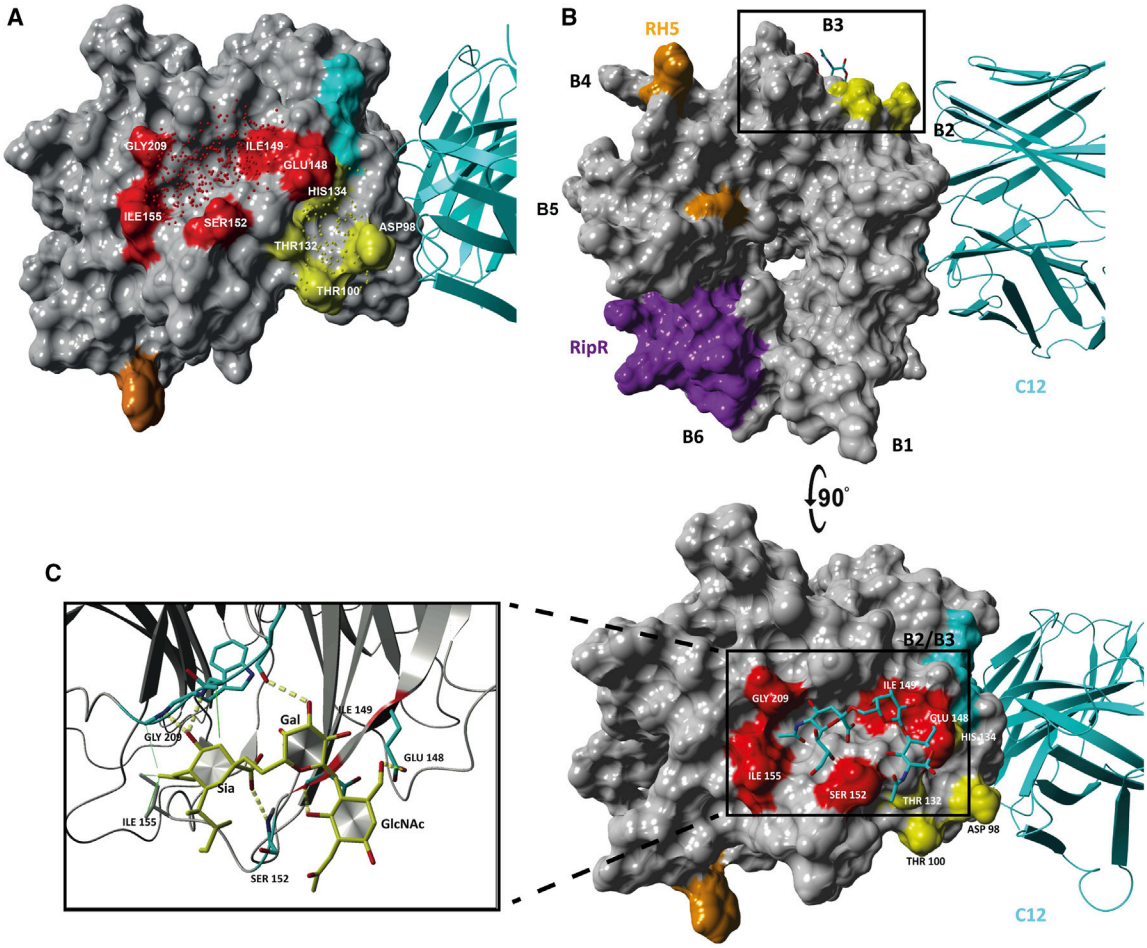

D

			C12 Antibody
WT	38.9 nM	1.89 nM	201 nM
G209A	33.9 nM	4.21 nM	307 nM
I155A	842 nM	25.4 nM	417 nM
S152A	54.2 μM	182 nM	561 nM
I149A	458 nM	No binding	277 nM
E148A	No binding	No binding	1.41 μM
H134A	31.9 nM	30.3 nM	421 nM
T132A	44.1 nM	16.9 nM	387 nM
T100A	41.4 nM	35.6 nM	294 nM
D98A	32.8 nM	11.7 nM	304 nM

Figure 2. Molecular model of *Pf*CyRPA in complex with mAb C12 and α2-6-SLN

(A) Non-biased identification of sialic-acid-recognizing sites on *Pf*CyRPA in complex with the parasite growth-inhibitory mAb C12 using the X-ray crystal structure of *Pf*CyRPA PDB: 5EZN (https://doi.org/10.2210/pdb5EZN/pdb). Lectin sites 1 (red) and 2 (yellow) as well as the *Pf*RipR (purple) and *Pf*Rh5 (orange) docking domains are marked.

(B) The view tilted by 90° includes the numbering of β-propeller blades B1–B6.

(C) Detailed view of the α2-6-SLN-Ac interaction with *Pf*CyRPA lectin site 1. Amino acids essential for glycan coordination (E148, I149, S152, I155, and G-209) in site 1 are labeled, and hydrogen bonds are marked (yellow lines). While bacterial sialidases contain three to five Asp boxes, *Pf*CyRPA contains only one (201-SHDKGETW-208),[11,16] which includes residues in the predicted lectin site 1.

(D) Affinities of *Pf*CyRPA wild type (WT) and alanine scanning mutants for the preferred glycan targets (α2-6-SLN-Ac and α2-6-Biant-Ac) and for mAb C12. Red and yellow indicate mutants in lectin site 1 and site 2, respectively; orange represents the alanine exchange mutant at position E148, which is part of both binding sites. SPR assay results are an average of at least three replicate experiments shown as average ± standard deviation in Table S3, with additional mutants that had no significant effect on CyRPA glycan recognition. SPR sensorgrams are shown in Figure S8.

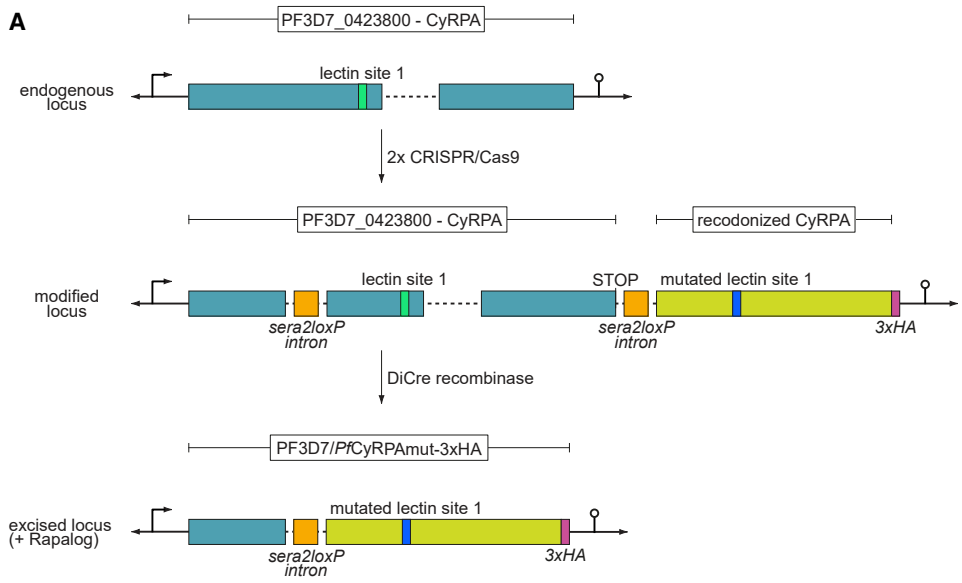

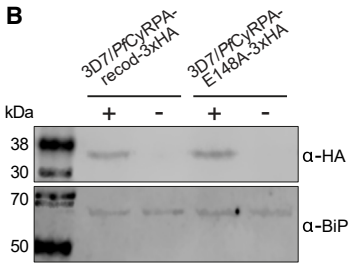

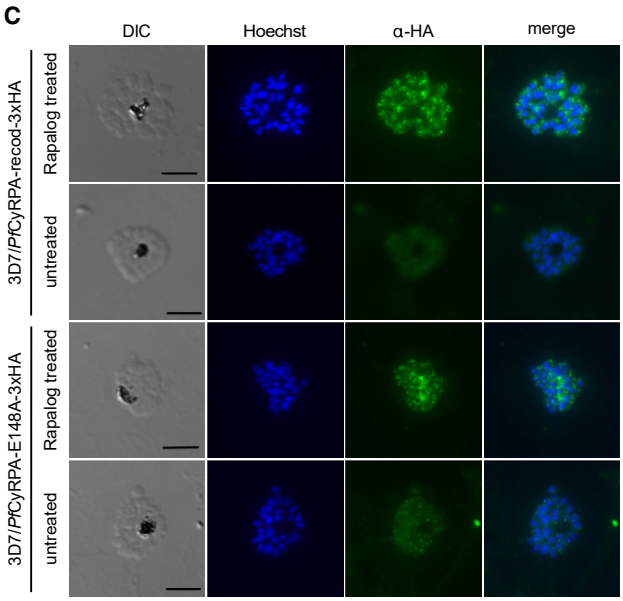

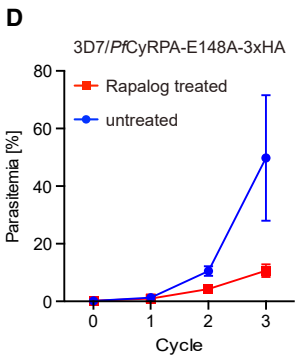

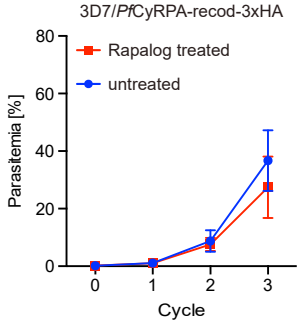

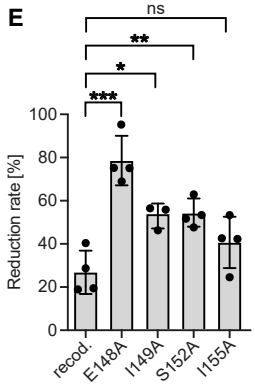

(legend on next page)

the human vs. non-human great ape forms of sialic acid, i.e., Neu5Ac vs. Neu5Gc (Figure 1A). Both injection of blood from *P. reichenowi*-infected chimpanzees into humans[29] and injection of blood from *P. falciparum*-infected humans into chimpanzees failed to produce a malaria infection. We hypothesize that this species specificity is a consequence of the adaptation of CyRPA, and potentially other structures,[30] to the human-specific and ape-predominant sialic acids.

*Pf*CyRPA and *Pr*CyRPA differ at one of the amino acid position of lectin site 1 involved in glycan binding (G209R). One other sequence difference is located close to the (E-148, Y-144, N-145, and N-146) binding loop (Y154H). To determine whether these two dimorphisms are impacting the difference in the specificity of *Pf*CyRPA vs. *Pr*CyRPA, Y154H and G209R were mutated in *Pf*CyRPA and analyzed for glycan binding (Figure 1B; Table S4). Remarkably, the *Pf*CyRPA$_{Y154H/G209R}$ double mutant, with the two *Pr*CyRPA lectin site polymorphisms, reverted to a *Pr*CyRPA lectin phenotype with an 11-fold higher K_D for the α2-6-Biant-Ac glycan and a 75-fold lower K_D for the α2-6-Biant-Gc glycan compared to the wild-type *Pf*CyRPA (Figure 1A). Therefore, as few as two point mutations in the *Pf*CyRPA progenitor may have been sufficient for the adaptation of *Pf*CyRPA toward high-affinity binding of human erythrocytes.

Lectin activity of *Pf*CyRPA is highly relevant for *P. falciparum* erythrocyte invasion

To further investigate the role of *Pf*CyRPA lectin activity during invasion, transgenic parasite lines, which enable conditional expression of mutant *Pf*CyRPA variants encoding point mutations in lectin site 1, were generated. Because of the essential nature of *Pf*CyRPA, a recently published 3D7 line, which allows the inducible expression of the DiCre recombinase,[31] was chosen for the generation of these parasites. Parasites were subjected to two rounds of CRISPR-Cas9-mediated genome editing, in order to introduce two *sera2loxPintron* sites[32] and a recodonized version of the *cyrpa* gene coding for the intended point mutations and a 3′-3xHA (hemagglutinin) tag, downstream of the endogenous *cyrpa* locus. Upon addition of Rapalog and the activation of the DiCre recombinase, a part of the endogenous *cyrpa* locus containing the predicted glycan-binding site 1 is excised and replaced by the recodonized version (see the genetic setup in Figure 3). Thus, these parasites enable the induced replacement of the endogenous *Pf*CyRPA with a mutant *Pf*CyRPA-mut-3xHA version and the analysis of resulting growth phenotypes. As expected from the SPR results described above, we observed that the E148A mutation resulted in the strongest growth inhibition assay phenotype. As a control, 3D7/*Pf*CyRPA-recodonized-3xHA parasites were generated that harbor the same genetic setup, but in these parasites, the endogenous *cyrpa* locus is replaced with a recodonized 3xHA-tagged wild-type copy upon Rapalog treatment. Successful gene editing was confirmed by PCR on genomic DNA (Figure S3). After induction with Rapalog, expression of HA-tagged *Pf*CyRPA variants was confirmed for both parasite lines using western blot experiments and immunofluorescence assays (IFAs) (Figures 3B and 3C). The western blots revealed successful expression of the *Pf*CyRPA-recodonized-3xHA and *Pf*CyRPA-E148A-3xHA fusion proteins upon addition of Rapalog. This was further confirmed by the IFA experiments, which showed the expected apical localization of the 3xHA-tagged *Pf*CyRPA fusion proteins in both parasite lines (Figure 3C). This suggested a correct processing and distribution of the tagged *Pf*CyRPA versions, excluding a negative effect of the 3xHA tag. Correct excision of the wild-type locus and replacement with the recodonized sequence upon induction with Rapalog was again confirmed by PCR using genomic DNA (Figure S4). Growth inhibition assays using flow cytometry showed a growth reduction of up to 80% in Rapalog-treated 3D7/*Pf*CyRPA-E148A-3xHA compared to a 20% reduction in Rapalog-treated 3D7/*Pf*CyRPA-recodonized-3xHA control parasites over three replication cycles (Figure 3D). This was in line with the observed loss of binding of the E148A mutant in the SPR studies (Figure 2D) and further confirmed an important function of the *Pf*CyRPA glycan-binding activity during parasite invasion. As expected, growth reduction by the I149A, S152A, and I155A amino acid exchanges, which had less impact on lectin activity (Figure 2D), was more moderate (Figure 3D).

*Pf*CyRPA lectin activity can be targeted with antibodies and small molecules

*Pf*CyRPA has previously been identified as a candidate malaria vaccine antigen by screening proteins expressed by merozoites for their ability to elicit parasite-inhibitory antibodies.[5,33] All three components of the invasion complex share the ability to induce invasion-inhibitory antibodies. Competition for antigen-binding assays have defined five anti-*Pf*CyRPA mAb epitope bins.[5,10] Most mAbs belonging to epitope bin B, which includes mAb C12, and epitope bin F interfere with α2-6-SLN binding to *Pf*CyRPA (Figure S5C).

Although members of both bins bind to the *Pf*CyRPA aa 26–251 fragment that comprises the entire lectin sites 1 and 2

Figure 3. Point mutation E148A in the lectin-binding site 1 of *Pf*CyRPA leads to growth inhibition of parasites

(A) Schematic overview of the two-step CRISPR-Cas9 genome-editing strategy used to generate the transgenic parasite lines, allowing the conditional expression of mutant 3xHA-tagged *Pf*CyRPA variants.

(B) Western blot analysis of 3xHA-tagged *Pf*CyRPA expression in the 3D7/*Pf*CyRPA-recodonized-3xHA (left) and 3D7/*Pf*CyRPA-E148A-3xHA (right) parasite lines either treated with Rapalog (+) or untreated control (−) (top). The Hsp70-like ER marker protein *Pf*BiP was used as a loading control (bottom).

(C) Anti-HA IFA experiments in fixed 3D7/*Pf*CyRPA-recodonized-3xHA (two top rows) and 3D7/*Pf*CyRPA-E148A-3xHA (two bottom rows), which were treated or untreated with Rapalog. DNA was counterstained using Hoechst. Scale bar: 5 μm.

(D) Growth curves of Rapalog-treated vs. untreated 3D7/*Pf*CyRPA-recodonized-3xHA (left) and 3D7/*Pf*CyRPA-E148A-3xHA (right) parasite lines. n = 4 biological replicates, error bars indicate standard deviation of the mean.

(E) Growth reduction rates of Rapalog-treated 3D7/*Pf*CyRPA-recodonized-3xHA and 3D7/*Pf*CyRPA-E148A-3xHA, 3D7/*Pf*CyRPA-I149A-3xHA, 3D7/*Pf*CyRPA-S152A-3xHA, and 3D7/*Pf*CyRPA-I155A-3xHA parasite lines. Growth rates of Rapalog-treated parasite lines were normalized to untreated control parasites of the corresponding parasite line. n = 4 biological replicates (except I149A, here n = 3), error bars indicate standard deviation of the mean. Unpaired t test, p = 0,0005, p = 0,0112, p = 0,0048, and p = 0,1256.

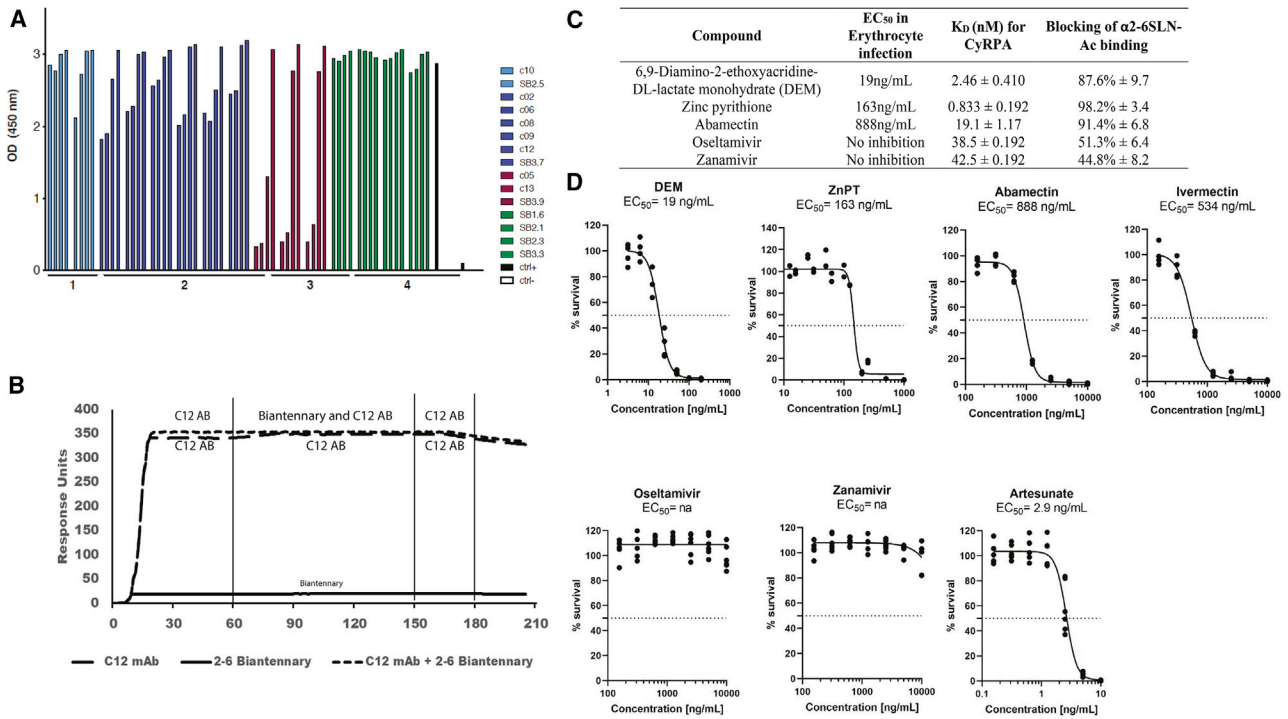

Compound	EC50 in Erythrocyte infection	KD (nM) for CyRPA	Blocking of α2-6SLN-Ac binding
6,9-Diamino-2-ethoxyacridine-DL-lactate monohydrate (DEM)	19ng/mL	2.46 ± 0.410	87.6% ± 9.7
Zinc pyrithione	163ng/mL	0.833 ± 0.192	98.2% ± 3.4
Abamectin	888ng/mL	19.1 ± 1.17	91.4% ± 6.8
Oseltamivir	No inhibition	38.5 ± 0.192	51.3% ± 6.4
Zanamivir	No inhibition	42.5 ± 0.192	44.8% ± 8.2

Figure 4. Antibodies and small molecules as competitors of the lectin activity of *Pf*CyRPA

(A) Antibodies that interfere with *Pf*RH5-*Pf*CyRPA interaction (C05, C13, and SB3.9) are non-inhibitory. ELISA plates were coated with recombinant *Pf*CyRPA; recombinant *Pf*RH5 and *Pf*CyRPA-specific mAbs (tested at 10, 5, 1, and 0.1 μg/mL) were used as competitors, and the anti-*Pf*RH5 mAb BS1.2 was used for detection. Wells incubated only with *Pf*RH5 served as positive control (black), and wells incubated with PBS and incubated with *Pf*RH5 alone served as negative control (white).

(B) Inhibition of α2-6-Biant-Ac binding to *Pf*CyRPA by mAb C12 determined by analysis of mAb C12 alone, α2-6-Biant-Ac alone, and the competition between α2-6-Biant-Ac and mAb C12 for the binding of *Pf*CyRPA. Blocking percentage and C10 mAb control are shown in Figures S5A and S5B. These are representative curves of experiments with 3 technical replicates, errors are one standard deviation of the mean.

(C) Activities of small molecules targeting the lectin activity of *Pf*CyRPA: parasite growth inhibition (EC50 indicates the concentration of the compound that is required to decrease parasite growth by 50%), binding affinity (K_D) for *Pf*CyRPA, and blocking activity for binding of α2-6-SLN-Ac to *Pf*CyRPA.

(D) Inhibition of parasite growth by identified small molecules. All erythrocyte assays are the average of 3 experiments. p values are ≤0.05.

(Figure 2), bin B and F mAbs do not compete with each other for antigen binding.[5,10] Only bin B mAbs bind to the PfCyRPA aa 26–181 fragment[11] that comprises the N-terminal part of lectin site 1 (148-EITISDYI-155) without the lectin site 1 sequence stretch around Gly-209 (Figure 2). This indicates that the epitope recognized by bin F mAbs is located further downstream of that of bin B mAbs. The structural analysis of *Pf*CyRPA-mAb c12 co-crystals[11] has in fact localized the mAb binding site adjacent to the N-terminal domain of lectin site 1 (Figure 2). The heavy-chain CDR3 residues Tyr-122 and Tyr-120 of mAb c12 form van der Waals interactions with the *Pf*CyRPA residues Tyr-144, Asn-145, and Asn-146,[11] which neighbor Glu-148 that is essential for α2-6-SLN binding (Figure 2). Interference with lectin activity does not seem to be essential for growth inhibition by anti-*Pf*CyRPA antibodies since mAbs belonging to epitope bins A and C, which do not interfere with carbohydrate binding, also have growth-inhibitory activity (Figure S5C). Similar results have been described for *Pf*RH5-specific mAbs, which include both epitope bins that inhibit *Pf*RH5 binding to basigin and mAbs that do not affect *Pf*RH5 binding to this erythrocyte ligand.[34] *Pf*CyRPA-specific mAbs belonging to epitope bins D and E (mAbs C05, C13, and SB3.9) inhibit binding of *Pf*CyRPA to *Pf*RH5 (Figure 4A) and were not growth inhibitory, reconfirming published data for both anti-*Pf*RH5 and anti-*Pf*CyRPA mAbs that inhibit the interaction between *Pf*CyRPA and *Pf*RH5 and lack parasite growth-inhibitory activity.[34,35] Since the *P. falciparum* invasion complex is preformed prior to its exposure on the parasite cell surface, contact surfaces between the individual invasion complex protein components are hidden and not accessible for antibodies. Protective immune responses are therefore primarily focused on domains 2, 3, and 4 comprising the *Pf*CyRPA lectin sites. Prototypical growth-inhibitory antibodies, like mAb C12[5,10] that interfere with glycan binding (Figure 4B) may have potential for passive immunotherapy. Focusing immune responses on such lectin-activity-inhibitory epitopes may be suitable to enhance malaria vaccine efficacy.

The neuraminidase of human influenza A virus, which shares the Asp-box sialidase signature motif with *Pf*CyRPA, plays a crucial role in infection and has been targeted in drug development approaches leading to the anti-influenza drugs zanamivir and oseltamivir.[36,37] Here, we performed SPR analyses and showed that these drugs bind with a lower affinity

($K_D \approx 40$ nM; Figure 4A) to *Pf*CyRPA than a candidate cellular receptor, α2-6-Biant-Ac ($K_D = 1.9$ nM), and exhibit no inhibitory activity in a *P. falciparum* parasite growth inhibition assay (Figures 4C and S6). To identify compounds capable of targeting the α2-6-SLN-Ac-binding activity of *Pf*CyRPA, we used a high-throughput SPR screening strategy[38–40] to interrogate a library of 3,142 drugs for binding to *Pf*CyRPA. Compounds that bound *Pf*CyRPA were then tested for their ability to block *Pf*CyRPA binding to α2-6-SLN-Ac in an SPR competition assay (Figures 4C and S6). These data showed that 6,9-diamino-2-ethoxyacridine-DL-lactate monohydrate (DEM; $K_D = 2.5$ nM), zinc pyrithione ($K_D = 0.8$ nM), and abamectin ($K_D = 19$ nM) bind *Pf*CyRPA with high affinity and can block α2-6-SLN-Ac binding to *Pf*CyRPA (Figures 4C and S6). Consistent with these observations, molecular docking studies of each of these blocking compounds with *Pf*CyRPA predicted binding to lectin site 1 (Figures S7A–S7C). All identified compounds that block *Pf*CyRPA lectin activity (DEM, abamectin, and zinc pyrithione) also inhibit parasite multiplication (Figure 4D), with DEM showing the most potent half-maximal effective concentration (EC_{50} = 19 ng/mL; Figures 4C and 4D). Taken together, these data provide proof of principle that small molecules blocking *Pf*CyRPA lectin activity represent a novel, invasion-blocking therapeutic approach to treating malaria.

It has been suggested that the function of *Pf*CyRPA is to tether the ternary invasion complex via a glycosylphosphatidylinositol (GPI) anchor on the merozoite surface.[7] However, the presence of GPI anchors on *Pf*CyRPA could not be confirmed.[41] Recent evidence indicates that the *Plasmodium thrombospondin*-related apical merozoite protein associates with the invasion complex and that its transmembrane domain anchors it to the parasite membrane.[42] In this study, we demonstrate that the essential function of *Pf*CyRPA lies in its lectin activity and that it binds to α2-6-linked Neu5Ac-containing glycans on human red blood cells. Amino acid residues relevant for *Pf*CyRPA lectin activity were predicted by molecular modeling, and the relevance of the identified residues was shown with both mutated recombinant proteins and transgenic parasites in erythrocyte invasion experiments. Utilizing sialic acid glycans as receptors is a feature common to a wide range of human pathogens, including the HA and sialidase of influenza A virus[43] and some adhesins and toxins of bacterial pathogens.[44] We also show that blocking the *Pf*CyRPA-glycan receptor interaction by *Pf*CyRPA lectin site-specific antibodies or small molecules can efficiently inhibit *P. falciparum* invasion of erythrocytes. Taken together, these findings indicate that targeting *Pf*CyRPA lectin activity with drugs, passive immunotherapy, or active immunization is a promising strategy to prevent and treat malaria.

Limitation of the study

We acknowledge that the prototype small molecules with lectin inhibitory activity identified here may have off-target effects that contribute to their anti-parasitic activity. Although this study provides new information with the discovery of *Pf*CyRPA lectin activity and the role of this activity in binding red blood cell glycans to promote erythrocyte invasion, the sequence of events and the precise role of other invasion complex proteins in this process are beyond the scope of this study and were not addressed. RH5 is found only in the *Laverania* subgenus and not in the closely related species *P. vivax* and *P. knowlesi.* While it has been shown that *Pk*CyRPA and *Pk*RIPR are essential for erythrocyte invasion, they do not form a complex with each other or with an RH5-like molecule.[45] Therefore, *P. vivax* and *P. knowlesi* do not require basigin as a host cell invasion receptor. *Pv*CyRPA and *Pk*CyRPA show limited sequence conservation to the newly defined lectin region of *Pf*CyRPA,[5] indicating that in these species, CyRPA may have adapted to recognize another human glycan than *Pf*CyRPA.

STAR★METHODS

Detailed methods are provided in the online version of this paper and include the following:

- KEY RESOURCES TABLE
- RESOURCE AVAILABILITY
  - Lead contact
  - Materials availability
  - Data and code availability
- EXPERIMENTAL MODEL AND STUDY PARTICIPANT DETAILS
- METHOD DETAILS
  - Expression and purification of *Pf*CyRPA and *Pr*CyRPA
  - Glycan array analysis of purified *Pf*CyRPA
  - Surface plasmon resonance (SPR) analysis of purified CyRPA
  - Docking of *N*-acetylneuraminic acid (Sia, Neu5Ac), and α2-6- and α2-3-sialyllactosamine (α2-6-SLN and α2-3-SLN) to *Pf*CyRPA
  - SPR analysis of the binding of *Pf*CyRPA to membranes of sialidase treated erythrocytes and of CRISPR/Cas9 knockouts
  - Immunofluorescence microscopy
  - Generation of transgenic *P. falciparum* lines
  - *P. falciparum* blood-stage culture
  - Proliferation assay of 3D7/*Pf*CyRPAmut lines
  - Western blot analysis of 3D7/*Pf*CyRPAmut parasites
  - SPR drug screening of *Pf*CyRPA
  - SPR competition assays of *Pf*CyRPA with antibodies and small molecules
  - *P. falciparum* blood-stage culture
  - *In vitro* growth inhibition assay (GIA)
  - Monoclonal antibodies (mAbs) specific for *Pf*CyRPA and *Pf*RH5
  - Cloning, expression, and purification of *Pf*RH5
  - *Pf*CyRPA-*Pf*RH5 mAb competition experiments
- QUANTIFICATION AND STATISTICAL ANALYSIS

SUPPLEMENTAL INFORMATION

Supplemental information can be found online at https://doi.org/10.1016/j.celrep.2024.114012.

ACKNOWLEDGMENTS

We thank Kate Fox (Erudito Editing) for editing a draft of this manuscript. We acknowledge Compounds Australia (www.compoundsaustralia.com) for their

provision of specialized compound management research services to the project. We want to thank Ellen Knuepfer and Anthony Holder for providing the 3D7 DiCre parasite line. This research was funded by the National Health and Medical Research Council (NHMRC) principal research fellowship 1138466 and investigator grant (L3) 2026356 (M.P.J.), the Unisciencia Foundation (G.P.), Fondation Botnar (G.P.), the state of Hamburg BWFGB LFF FV-069 (S.B., T.-W.G., and M.F.), and the Swiss National Science Foundation (grant number 310030_200683) (N.M.B.B.).

AUTHOR CONTRIBUTIONS

Conceptualization, C.J.D., M.P.J., M.F., C.G., N.M.B.B., and G.P.; methodology, M.F., T.-W.G., C.G., and N.M.B.B.; provided resources and materials, C.T.F. and M.T.D.; data acquisition, C.J.D., P.F., T.H., J.H., L.K.S., C.F., J.P., F.E.-C.J., A.S., J.-P.D., M.T., S.B., and L.S.; data analysis, C.J.D., P.F., T.H., J.H., L.K.S., C.F., J.P., F.E.-C.J., A.S., J.-P.D., M.T., M.P.J., G.P., S.B., and M.F.; funding acquisition, M.P.J., G.P., and M.F.; supervision, C.J.D., T.H., M.P.J., G.P., M.F., and C.G.; writing – original draft, C.J.D., T.H., M.P.J., G.P., and M.F.; writing – review & editing, C.J.D., P.F., T.H., J.H., L.K.S., C.F., J.P., F.E.-C.J., A.S., J.-P.D., T.-W.G., M.T., M.P.J., G.P., and M.F.

DECLARATION OF INTERESTS

C.J.D., M.P.J., and G.P. are inventors on a patent related to this publication.

Received: July 27, 2023
Revised: December 15, 2023
Accepted: March 13, 2024

REFERENCES

1. Tham, W.H., Healer, J., and Cowman, A.F. (2012). Erythrocyte and reticulocyte binding-like proteins of Plasmodium falciparum. Trends Parasitol. *28*, 23–30. https://doi.org/10.1016/j.pt.2011.10.002.
2. Baum, J., Chen, L., Healer, J., Lopaticki, S., Boyle, M., Triglia, T., Ehlgen, F., Ralph, S.A., Beeson, J.G., and Cowman, A.F. (2009). Reticulocyte-binding protein homologue 5 - an essential adhesin involved in invasion of human erythrocytes by Plasmodium falciparum. Int. J. Parasitol. *39*, 371–380. https://doi.org/10.1016/j.ijpara.2008.10.006.
3. Beeson, J.G., Drew, D.R., Boyle, M.J., Feng, G., Fowkes, F.J.I., and Richards, J.S. (2016). Merozoite surface proteins in red blood cell invasion, immunity and vaccines against malaria. FEMS Microbiol. Rev. *40*, 343–372. https://doi.org/10.1093/femsre/fuw001.
4. Cowman, A.F., Tonkin, C.J., Tham, W.H., and Duraisingh, M.T. (2017). The Molecular Basis of Erythrocyte Invasion by Malaria Parasites. Cell Host Microbe *22*, 232–245. https://doi.org/10.1016/j.chom.2017.07.003.
5. Dreyer, A.M., Matile, H., Papastogiannidis, P., Kamber, J., Favuzza, P., Voss, T.S., Wittlin, S., and Pluschke, G. (2012). Passive immunoprotection of Plasmodium falciparum-infected mice designates the CyRPA as candidate malaria vaccine antigen. J. Immunol. *188*, 6225–6237. https://doi.org/10.4049/jimmunol.1103177.
6. Chen, L., Lopaticki, S., Riglar, D.T., Dekiwadia, C., Uboldi, A.D., Tham, W.H., O'Neill, M.T., Richard, D., Baum, J., Ralph, S.A., and Cowman, A.F. (2011). An EGF-like protein forms a complex with PfRh5 and is required for invasion of human erythrocytes by Plasmodium falciparum. PLoS Pathog. *7*, e1002199. https://doi.org/10.1371/journal.ppat.1002199.
7. Reddy, K.S., Amlabu, E., Pandey, A.K., Mitra, P., Chauhan, V.S., and Gaur, D. (2015). Multiprotein complex between the GPI-anchored CyRPA with PfRH5 and PfRipr is crucial for Plasmodium falciparum erythrocyte invasion. Proc. Natl. Acad. Sci. USA *112*, 1179–1184. https://doi.org/10.1073/pnas.1415466112.
8. Wong, W., Huang, R., Menant, S., Hong, C., Sandow, J.J., Birkinshaw, R.W., Healer, J., Hodder, A.N., Kanjee, U., Tonkin, C.J., et al. (2019). Structure of Plasmodium falciparum Rh5-CyRPA-Ripr invasion complex. Nature *565*, 118–121. https://doi.org/10.1038/s41586-018-0779-6.
9. Douglas, A.D., Williams, A.R., Knuepfer, E., Illingworth, J.J., Furze, J.M., Crosnier, C., Choudhary, P., Bustamante, L.Y., Zakutansky, S.E., Awuah, D.K., et al. (2014). Neutralization of Plasmodium falciparum merozoites by antibodies against PfRH5. J. Immunol. *192*, 245–258. https://doi.org/10.4049/jimmunol.1302045.
10. Favuzza, P., Blaser, S., Dreyer, A.M., Riccio, G., Tamborrini, M., Thoma, R., Matile, H., and Pluschke, G. (2016). Generation of Plasmodium falciparum parasite-inhibitory antibodies by immunization with recombinantly-expressed CyRPA. Malar. J. *15*, 161. https://doi.org/10.1186/s12936-016-1213-x.
11. Favuzza, P., Guffart, E., Tamborrini, M., Scherer, B., Dreyer, A.M., Rufer, A.C., Erny, J., Hoernschemeyer, J., Thoma, R., Schmid, G., et al. (2017). Structure of the malaria vaccine candidate antigen CyRPA and its complex with a parasite invasion inhibitory antibody. Elife *6*, e20383. https://doi.org/10.7554/eLife.20383.
12. Healer, J., Chiu, C.Y., and Hansen, D.S. (2018). Mechanisms of naturally acquired immunity to P. falciparum and approaches to identify merozoite antigen targets. Parasitology *145*, 839–847. https://doi.org/10.1017/S0031182017001949.
13. Farrell, B., Alam, N., Hart, M.N., Jamwal, A., Ragotte, R.J., Walters-Morgan, H., Draper, S.J., Knuepfer, E., and Higgins, M.K. (2024). The PfRCR complex bridges malaria parasite and erythrocyte during invasion. Nature *625*, 578–584. https://doi.org/10.1038/s41586-023-06856-1.
14. Crosnier, C., Bustamante, L.Y., Bartholdson, S.J., Bei, A.K., Theron, M., Uchikawa, M., Mboup, S., Ndir, O., Kwiatkowski, D.P., Duraisingh, M.T., et al. (2011). Basigin is a receptor essential for erythrocyte invasion by Plasmodium falciparum. Nature *480*, 534–537. https://doi.org/10.1038/nature10606.
15. Nagaoka, H., Kanoi, B.N., Ntege, E.H., Aoki, M., Fukushima, A., Tsuboi, T., and Takashima, E. (2020). Antibodies against a short region of PfRipr inhibit Plasmodium falciparum merozoite invasion and PfRipr interaction with Rh5 and SEMA7A. Sci. Rep. *10*, 6573. https://doi.org/10.1038/s41598-020-63611-6.
16. Chen, L., Xu, Y., Wong, W., Thompson, J.K., Healer, J., Goddard-Borger, E.D., Lawrence, M.C., and Cowman, A.F. (2017). Structural basis for inhibition of erythrocyte invasion by antibodies to Plasmodium falciparum protein CyRPA. Elife *6*, e21347. https://doi.org/10.7554/eLife.21347.
17. Waespy, M., Gbem, T.T., Elenschneider, L., Jeck, A.P., Day, C.J., Hartley-Tassell, L., Bovin, N., Tiralongo, J., Haselhorst, T., and Kelm, S. (2015). Carbohydrate Recognition Specificity of Trans-sialidase Lectin Domain from Trypanosoma congolense. PLoS Neglected Trop. Dis. *9*, e0004120. https://doi.org/10.1371/journal.pntd.0004120.
18. Bewley, C.A. (2008). Illuminating the switch in influenza viruses. Nat. Biotechnol. *26*, 60–62. https://doi.org/10.1038/nbt0108-60.
19. Sparrow, R.L., Healey, G., Patton, K.A., and Veale, M.F. (2006). Red blood cell age determines the impact of storage and leukocyte burden on cell adhesion molecules, glycophorin A and the release of annexin V. Transfus. Apher. Sci. *34*, 15–23. https://doi.org/10.1016/j.transci.2005.09.006.
20. Muramatsu, T. (2016). Basigin (CD147), a multifunctional transmembrane glycoprotein with various binding partners. J. Biochem. *159*, 481–490. https://doi.org/10.1093/jb/mvv127.
21. Parkkinen, J., Rogers, G.N., Korhonen, T., Dahr, W., and Finne, J. (1986). Identification of the O-linked sialyloligosaccharides of glycophorin A as the erythrocyte receptors for S-fimbriated Escherichia coli. Infect. Immun. *54*, 37–42. https://doi.org/10.1128/iai.54.1.37-42.1986.
22. Bai, Y., Huang, W., Ma, L.T., Jiang, J.L., and Chen, Z.N. (2014). Importance of N-glycosylation on CD147 for its biological functions. Int. J. Mol. Sci. *15*, 6356–6377. https://doi.org/10.3390/ijms15046356.
23. Hayakawa, T., Aki, I., Varki, A., Satta, Y., and Takahata, N. (2006). Fixation of the human-specific CMP-N-acetylneuraminic acid hydroxylase

pseudogene and implications of haplotype diversity for human evolution. Genetics *172*, 1139–1146. https://doi.org/10.1534/genetics.105.046995.

24. Muchmore, E.A., Diaz, S., and Varki, A. (1998). A structural difference between the cell surfaces of humans and the great apes. Am. J. Phys. Anthropol. *107*, 187–198. https://doi.org/10.1002/(SICI)1096-8644(199810)107:2<187::AID-AJPA5>3.0.CO;2-S.

25. Altman, M.O., and Gagneux, P. (2019). Absence of Neu5Gc and Presence of Anti-Neu5Gc Antibodies in Humans-An Evolutionary Perspective. Front. Immunol. *10*, 789. https://doi.org/10.3389/fimmu.2019.00789.

26. Martin, M.J., Rayner, J.C., Gagneux, P., Barnwell, J.W., and Varki, A. (2005). Evolution of human-chimpanzee differences in malaria susceptibility: relationship to human genetic loss of N-glycolylneuraminic acid. Proc. Natl. Acad. Sci. USA *102*, 12819–12824. https://doi.org/10.1073/pnas.0503819102.

27. Jaskiewicz, E., Jodłowska, M., Kaczmarek, R., and Zerka, A. (2019). Erythrocyte glycophorins as receptors for Plasmodium merozoites. Parasites Vectors *12*, 317. https://doi.org/10.1186/s13071-019-3575-8.

28. Shewell, L.K., Harvey, R.M., Higgins, M.A., Day, C.J., Hartley-Tassell, L.E., Chen, A.Y., Gillen, C.M., James, D.B.A., Alonzo, F., 3rd, Torres, V.J., et al. (2014). The cholesterol-dependent cytolysins pneumolysin and streptolysin O require binding to red blood cell glycans for hemolytic activity. Proc. Natl. Acad. Sci. USA *111*, E5312–E5320. https://doi.org/10.1073/pnas.1412703111.

29. Rodhain, J. (1939). Les plasmodiums des anthropoides de l'Afrique centrale et leurs relations avec les plasmodiums humains. Ann. Soc. Belge Med. Trop. *19*, 563–572.

30. Proto, W.R., Siegel, S.V., Dankwa, S., Liu, W., Kemp, A., Marsden, S., Zenonos, Z.A., Unwin, S., Sharp, P.M., Wright, G.J., et al. (2019). Adaptation of Plasmodium falciparum to humans involved the loss of an ape-specific erythrocyte invasion ligand. Nat. Commun. *10*, 4512. https://doi.org/10.1038/s41467-019-12294-3.

31. Knuepfer, E., Napiorkowska, M., van Ooij, C., and Holder, A.A. (2017). Generating conditional gene knockouts in Plasmodium - a toolkit to produce stable DiCre recombinase-expressing parasite lines using CRISPR/Cas9. Sci. Rep. *7*, 3881. https://doi.org/10.1038/s41598-017-03984-3.

32. Jones, M.L., Das, S., Belda, H., Collins, C.R., Blackman, M.J., and Treeck, M. (2016). A versatile strategy for rapid conditional genome engineering using loxP sites in a small synthetic intron in Plasmodium falciparum. Sci. Rep. *6*, 21800. https://doi.org/10.1038/srep21800.

33. Dreyer, A.M., Beauchamp, J., Matile, H., and Pluschke, G. (2010). An efficient system to generate monoclonal antibodies against membrane-associated proteins by immunisation with antigen-expressing mammalian cells. BMC Biotechnol. *10*, 87. https://doi.org/10.1186/1472-6750-10-87.

34. Alanine, D.G.W., Quinkert, D., Kumarasingha, R., Mehmood, S., Donnellan, F.R., Minkah, N.K., Dadonaite, B., Diouf, A., Galaway, F., Silk, S.E., et al. (2019). Human Antibodies that Slow Erythrocyte Invasion Potentiate Malaria-Neutralizing Antibodies. Cell *178*, 216–228.e21. https://doi.org/10.1016/j.cell.2019.05.025.

35. Ragotte, R.J., Pulido, D., Lias, A.M., Quinkert, D., Alanine, D.G.W., Jamwal, A., Davies, H., Nacer, A., Lowe, E.D., Grime, G.W., et al. (2022). Heterotypic interactions drive antibody synergy against a malaria vaccine candidate. Nat. Commun. *13*, 933. https://doi.org/10.1038/s41467-022-28601-4.

36. Eisenberg, E.J., Bidgood, A., and Cundy, K.C. (1997). Penetration of GS4071, a novel influenza neuraminidase inhibitor, into rat bronchoalveolar lining fluid following oral administration of the prodrug GS4104. Antimicrob. Agents Chemother. *41*, 1949–1952. https://doi.org/10.1128/AAC.41.9.1949.

37. von Itzstein, M., Wu, W.Y., Kok, G.B., Pegg, M.S., Dyason, J.C., Jin, B., Van Phan, T., Smythe, M.L., White, H.F., Oliver, S.W., et al. (1993). Rational design of potent sialidase-based inhibitors of influenza virus replication. Nature *363*, 418–423. https://doi.org/10.1038/363418a0.

38. Day, C.J., Bailly, B., Guillon, P., Dirr, L., Jen, F.E.C., Spillings, B.L., Mak, J., von Itzstein, M., Haselhorst, T., and Jennings, M.P. (2021). Multidisciplinary Approaches Identify Compounds that Bind to Human ACE2 or SARS-CoV-2 Spike Protein as Candidates to Block SARS-CoV-2-ACE2 Receptor Interactions. mBio *12*, e03681-20. https://doi.org/10.1128/mBio.03681-20.

39. Poole, J., Day, C.J., Haselhorst, T., Jen, F.E.C., Torres, V.J., Edwards, J.L., and Jennings, M.P. (2020). Repurposed Drugs That Block the Gonococcus-Complement Receptor 3 Interaction Can Prevent and Cure Gonococcal Infection of Primary Human Cervical Epithelial Cells. mBio *11*, e03046-19. https://doi.org/10.1128/mBio.03046-19.

40. Shewell, L.K., Day, C.J., Jen, F.E.C., Haselhorst, T., Atack, J.M., Reijneveld, J.F., Everest-Dass, A., James, D.B.A., Boguslawski, K.M., Brouwer, S., et al. (2020). All major cholesterol-dependent cytolysins use glycans as cellular receptors. Sci. Adv. *6*, eaaz4926. https://doi.org/10.1126/sciadv.aaz4926.

41. Volz, J.C., Yap, A., Sisquella, X., Thompson, J.K., Lim, N.T.Y., Whitehead, L.W., Chen, L., Lampe, M., Tham, W.H., Wilson, D., et al. (2016). Essential Role of the PfRh5/PfRipr/CyRPA Complex during Plasmodium falciparum Invasion of Erythrocytes. Cell Host Microbe *20*, 60–71. https://doi.org/10.1016/j.chom.2016.06.004.

42. Scally, S.W., Triglia, T., Evelyn, C., Seager, B.A., Pasternak, M., Lim, P.S., Healer, J., Geoghegan, N.D., Adair, A., Tham, W.H., et al. (2022). PCRCR complex is essential for invasion of human erythrocytes by Plasmodium falciparum. Nat. Microbiol. *7*, 2039–2053. https://doi.org/10.1038/s41564-022-01261-2.

43. Ng, P.S.K., Böhm, R., Hartley-Tassell, L.E., Steen, J.A., Wang, H., Lukowski, S.W., Hawthorne, P.L., Trezise, A.E.O., Coloe, P.J., Grimmond, S.M., et al. (2014). Ferrets exclusively synthesize Neu5Ac and express naturally humanized influenza A virus receptors. Nat. Commun. *5*, 5750. https://doi.org/10.1038/ncomms6750.

44. Poole, J., Day, C.J., von Itzstein, M., Paton, J.C., and Jennings, M.P. (2018). Glycointeractions in bacterial pathogenesis. Nat. Rev. Microbiol. *16*, 440–452. https://doi.org/10.1038/s41579-018-0007-2.

45. Knuepfer, E., Wright, K.E., Kumar Prajapati, S., Rawlinson, T.A., Mohring, F., Koch, M., Lyth, O.R., Howell, S.A., Villasis, E., Snijders, A.P., et al. (2019). Divergent roles for the RH5 complex components, CyRPA and RIPR in human-infective malaria parasites. PLoS Pathog. *15*, e1007809. https://doi.org/10.1371/journal.ppat.1007809.

46. Kurita, R., Funato, K., Abe, T., Watanabe, Y., Shiba, M., Tadokoro, K., Nakamura, Y., Nagai, T., and Satake, M. (2019). Establishment and characterization of immortalized erythroid progenitor cell lines derived from a common cell source. Exp. Hematol. *69*, 11–16. https://doi.org/10.1016/j.exphem.2018.10.005.

47. Scully, E.J., Shabani, E., Rangel, G.W., Grüring, C., Kanjee, U., Clark, M.A., Chaand, M., Kurita, R., Nakamura, Y., Ferreira, M.U., and Duraisingh, M.T. (2019). Generation of an immortalized erythroid progenitor cell line from peripheral blood: A model system for the functional analysis of Plasmodium spp. invasion. Am. J. Hematol. *94*, 963–974. https://doi.org/10.1002/ajh.25543.

48. Trakarnsanga, K., Griffiths, R.E., Wilson, M.C., Blair, A., Satchwell, T.J., Meinders, M., Cogan, N., Kupzig, S., Kurita, R., Nakamura, Y., et al. (2017). An immortalized adult human erythroid line facilitates sustainable and scalable generation of functional red cells. Nat. Commun. *8*, 14750. https://doi.org/10.1038/ncomms14750.

49. Xiao, Z., Wan, J., Nur, A.A., Dou, P., Mankin, H., Liu, T., and Ouyang, Z. (2018). Targeting CD44 by CRISPR-Cas9 in Multi-Drug Resistant Osteosarcoma Cells. Cell. Physiol. Biochem. *51*, 1879–1893. https://doi.org/10.1159/000495714.

50. Kanjee, U., Grüring, C., Chaand, M., Lin, K.M., Egan, E., Manzo, J., Jones, P.L., Yu, T., Barker, R., Jr., Weekes, M.P., and Duraisingh, M.T. (2017). CRISPR/Cas9 knockouts reveal genetic interaction between strain-transcendent erythrocyte determinants of Plasmodium falciparum invasion.

Proc. Natl. Acad. Sci. USA *114*, E9356–E9365. https://doi.org/10.1073/pnas.1711310114.

51. Satchwell, T.J., Wright, K.E., Haydn-Smith, K.L., Sánchez-Román Terán, F., Moura, P.L., Hawksworth, J., Frayne, J., Toye, A.M., and Baum, J. (2019). Genetic manipulation of cell line derived reticulocytes enables dissection of host malaria invasion requirements. Nat. Commun. *10*, 3806. https://doi.org/10.1038/s41467-019-11790-w.
52. Trott, O., and Olson, A.J. (2010). AutoDock Vina: improving the speed and accuracy of docking with a new scoring function, efficient optimization, and multithreading. J. Comput. Chem. *31*, 455–461. https://doi.org/10.1002/jcc.21334.
53. Krieger, E., Koraimann, G., and Vriend, G. (2002). Increasing the precision of comparative models with YASARA NOVA–a self-parameterizing force field. Proteins *47*, 393–402. https://doi.org/10.1002/prot.10104.
54. Brinkman, E.K., Chen, T., Amendola, M., and van Steensel, B. (2014). Easy quantitative assessment of genome editing by sequence trace decomposition. Nucleic Acids Res. *42*, e168. https://doi.org/10.1093/nar/gku936.
55. Schindelin, J., Arganda-Carreras, I., Frise, E., Kaynig, V., Longair, M., Pietzsch, T., Preibisch, S., Rueden, C., Saalfeld, S., Schmid, B., et al. (2012). Fiji: an open-source platform for biological-image analysis. Nat. Methods *9*, 676–682. https://doi.org/10.1038/nmeth.2019.
56. DuMont, A.L., Yoong, P., Day, C.J., Alonzo, F., McDonald, W.H., Jennings, M.P., and Torres, V.J. (2013). Staphylococcus aureus LukAB cytotoxin kills human neutrophils by targeting the CD11b subunit of the integrin Mac-1. Proc. Natl. Acad. Sci. USA *110*, 10794–10799. https://doi.org/10.1073/pnas.1305121110.
57. Wang, Z., Sun, H., Yao, X., Li, D., Xu, L., Li, Y., Tian, S., and Hou, T. (2016). Comprehensive evaluation of ten docking programs on a diverse set of protein-ligand complexes: the prediction accuracy of sampling power and scoring power. Phys. Chem. Chem. Phys. *18*, 12964–12975. https://doi.org/10.1039/c6cp01555g.
58. Filarsky, M., Fraschka, S.A., Niederwieser, I., Brancucci, N.M.B., Carrington, E., Carrió, E., Moes, S., Jenoe, P., Bártfai, R., and Voss, T.S. (2018). GDV1 induces sexual commitment of malaria parasites by antagonizing HP1-dependent gene silencing. Science *359*, 1259–1263. https://doi.org/10.1126/science.aan6042.
59. Thomas, J.A., Collins, C.R., Das, S., Hackett, F., Graindorge, A., Bell, D., Deu, E., and Blackman, M.J. (2016). Development and Application of a Simple Plaque Assay for the Human Malaria Parasite Plasmodium falciparum. PLoS One *11*, e0157873. https://doi.org/10.1371/journal.pone.0157873.
60. Matile, H., and Pink, J.R. (1990). Plasmodium falciparum malaria parasite cultures and their use in immunology. In Immunological Methods, I. Lefkovits and B. Pernis, eds. (Academic Press), pp. 221–234.
61. Dorn, A., Stoffel, R., Matile, H., Bubendorf, A., and Ridley, R.G. (1995). Malarial haemozoin/beta-haematin supports haem polymerization in the absence of protein. Nature *374*, 269–271. https://doi.org/10.1038/374269a0.
62. Lambros, C., and Vanderberg, J.P. (1979). Synchronization of Plasmodium falciparum erythrocytic stages in culture. J. Parasitol. *65*, 418–420.
63. Coll, R.C., Hill, J.R., Day, C.J., Zamoshnikova, A., Boucher, D., Massey, N.L., Chitty, J.L., Fraser, J.A., Jennings, M.P., Robertson, A.A.B., and Schroder, K. (2019). MCC950 directly targets the NLRP3 ATP-hydrolysis motif for inflammasome inhibition. Nat. Chem. Biol. *15*, 556–559. https://doi.org/10.1038/s41589-019-0277-7.

STAR★METHODS

KEY RESOURCES TABLE

REAGENT or RESOURCE	SOURCE	IDENTIFIER
Antibodies		
Mouse anti-His IgG	Cell Signaling Technology	Cat# 2366, RRID: AB_2115719
Alexa 555 rabbit anti-mouse IgG	Thermo Fisher Scientific	Cat# A-21427, RRID: AB_2535848
Alexa 555 goat anti-rabbit IgG	Thermo Fisher Scientific	Cat# A-21428, RRID: AB_2535849
REAfinity™ CD44-APC	Miltenyi Biotec	Cat# 130-113-900, RRID: AB_2726391
REAfinity™ CD147-VioBlue	Miltenyi Biotec	Cat# 130-104-537, RRID: AB_2655192
Mouse anti-*Pf*CyRPA mAb C10	Dreyer et al.[5]	N/A
Bacterial and virus strains		
E. coli strain Top10	Life Technologies	N/A
Chemicals, peptides, and recombinant proteins		
PfCyRPA	Dreyer et al.[5]	*P. falciparum* PF3D7_0423800
PrCyRPA	Favuzza et al.[10]	*P. reichenowi* PRCDC_0421000
Experimental models: Cell lines		
FreeStyle 293 F cells	Thermo Fisher Scientific	R790-07 RRID: CVCL_D603
BF, immortalized erythroid human cell line	Kurita et al., Scully et al. and Trakarnsanga et al.[46–48]	N/A
Recombinant DNA		
pcDNA3.1_BVM_CyRPA(29–362)_His6	Favuzza et al.[11]	Addgene
CD44 sgRNA 1	Xiao et al.[49]	Integrated DNA Technologies
CD44 sgRNA 2	Kanjee et al.[50]	Integrated DNA Technologies
Basigin sgRNA 1	Kanjee et al.[50]	Integrated DNA Technologies
Basigin sgRNA 2	Satchwell et al.[51]	Integrated DNA Technologies
Software and algorithms		
MAPIX software package	Mapix	RRID: SCR_002723
Microsoft Office 365 Excel	Microsoft	RRID: SCR_016137
Biacore S200 system control software	Cytiva	
Biacore S200 evaluation software package	Cytiva	RRID: SCR_015936
AutoDock Vina protocol	Trott, and Olson[52]	RRID: SCR_011958
YASARA structure molecular modeling package (Ver. 16.46)	Krieger et al.[53]	RRID: SCR_017591
GLYCAM carbohydrate builder	Woods Group. (2005–2020) GLYCAM Web. (http://glycam.org)	RRID: SCR_018260
FlowJo software	BD Life Sciences	RRID: SCR_008520
TIDE analysis	Brinkman et al.[54]	https://tide.nki.nl; RRID: SCR_023704
Biacore T200 system control software	Cytiva	RRID: SCR_019718
Biacore T200 evaluation software package	Cytiva	RRID: SCR_019718
ICY bio image analysis software	icy	RRID: SCR_010587
FIJI software (Version 2.1.0 for Mac OS X)	Schindelin et al.[55]	RRID: SCR_002285
Other		
*Pf*CyRPA X-ray crystal structure	Favuzza et al.[11]	PDB: 5EZN (https://doi.org/10.2210/pdb5EZN/pdb)

RESOURCE AVAILABILITY

Lead contact

Further information and requests for resources and reagents will be fulfilled by the lead contact, Gerd Pluschke (gerd.pluschke@swisstph.ch.

Materials availability

This study did not generate new unique reagents.

Data and code availability

- All data reported in this paper will be shared by the lead contact upon request.
- This paper does not report original code.
- Any additional information required to reanalyze the data reported in this paper is available from the lead contact upon request.

EXPERIMENTAL MODEL AND STUDY PARTICIPANT DETAILS

Primary erythrocytes were obtained from the Swiss Red Cross (Switzerland); all information on the donor is kept anonymous.

METHOD DETAILS

Expression and purification of *Pf*CyRPA and *Pr*CyRPA

Recombinant secreted *P. falciparum* and *P. reichenowi* wild type and mutant CyRPA were expressed essentially as described previously,[5,10] as histidine-tagged fusion proteins comprising CyRPA sequences without the signal sequence (aa 1–28). In brief, the expression vector pcDNA3.1_BVM_CyRPA(29–362)_His6[11] was used to express the codon-optimized *P. falciparum* PF3D7_0423800 or *P. reichenowi* PRCDC_0421000 sequence as a fusion protein with the bee-venom melittin signal sequence to allow for secretion of the C-terminally His6-tagged *Pf*CyRPA into the cultivation medium. Expression vectors coding for *Pf*CyRPA single amino acid variants were generated by site-directed mutagenesis (GenScript Biotech, Leiden, Netherlands). Plasmids were amplified in *E. coli* strain Top10 (Life Technologies) grown in LB medium under 100 mg/mL ampicillin selection and used for transfection of FreeStyle 293 F cells (Thermo Fisher Scientific, R790-07 RRID:CVCL_D603), a variant of human embryonic kidney HEK cells. Cells were cultured in suspension in serum-free medium (FreeStyle 293 Expression Medium, Thermo Fisher Scientific, Waltham, MA, USA). At 72 h post-transfection, cells were removed by filtration, the supernatant was concentrated and the His6-tagged recombinant fusion proteins were purified by immobilized metal ion affinity chromatography on a HisTrap HP column (Cytiva).

Glycan array analysis of purified *Pf*CyRPA

Glycan array slides were printed as previously described.[17] Glycan array binding experiments were performed and analyzed as previously described.[28] Briefly, 2 μg of *Pf*CyRPA in 1xPBS containing 1 mM $MgCl_2$ and 1 mM $CaCl_2$ was pre-complexed at room temperature with mouse anti-His antibody (Cell Signaling Technology Cat# 2366, RRID:AB_2115719), Alexa 555 rabbit anti-mouse IgG (Thermo Fisher Scientific Cat# A-21427, RRID:AB_2535848) and Alexa 555 goat anti-rabbit IgG (Thermo Fisher Scientific Cat# A-21428, RRID:AB_2535849) and then pre-blocked (1% bovine serum albumin in PBS) for 15 min. Slides were washed three times for 2 min in 1xPBS, dried by centrifugation, scanned with Innopsys Innoscan 1100AL and analyzed using the MAPIX software package Mapix (RRID:SCR_002723) and Microsoft Excel (RRID:SCR_016137) for statistical analysis (Student's unpaired t test of fluorescence of the background spots vs. fluorescence of the glycan printed spots). Results were obtained from three arrays and a total of 12 data points per glycan. See Table S1 for the full list of glycans and Table S6 for the MIRAGE compliant array methods for the production and quality control of the glycan arrays utilized.

Surface plasmon resonance (SPR) analysis of purified CyRPA

Purified *Pf*CyRPA and *Pr*CyRPA wild type and point mutants at 50 μg/mL were immobilized onto a series S CM5 chip using a Biacore S200 system (Cytiva) at a flow rate of 5 μL/min for 10 min in sodium acetate pH 4.0 at 25°C using a modification of a previously described method.[56] Initial glycan screens were performed at a range of 160 nM to 100 μM, with the range refined for each interaction with a minimum concentration range of 1.6 nM–1 μM (α2-6SLN compounds) performed. Antibody screening was performed with a concentration range of 1.6 nM–1 μM. SPR sensorgrams are shown in Figure S8.

Docking of *N*-acetylneuraminic acid (Sia, Neu5Ac), and α2-6- and α2-3-sialyllactosamine (α2-6-SLN and α2-3-SLN) to *Pf*CyRPA

To evaluate the potential *N*-acetylneuraminic acid (Neu5Ac) binding site, a docking experiment of *Pf*CyRPA was performed using the AutoDock Vina protocol (RRID:SCR_011958).[52] The X-ray crystal structure of *Pf*CyRPA PDB: 5EZN (https://doi.org/10.2210/pdb5EZN/pdb)[11] was used for docking. It has been shown that AutoDock Vina has the highest scoring power among commercial and academic molecular docking programs[57] implemented in the YASARA (RRID:SCR_017591) structure molecular modeling package (Ver. 16.46).[53] A blind docking experiment of Neu5Ac-αOH was set up using the entire *Pf*CyrRPA protein as a potential binding site (grid size 72.18 × 88.61 × 67.11 Å). Neu5Ac-αOH was generated using GLYCAM carbohydrate builder [Woods Group. (2005–2020) GLYCAM Web. Complex Carbohydrate Research Center, University of Georgia, Athens, GA (http://glycam.org) GLYCAM-Web (RRID:SCR_018260)]. This initial blind docking procedure for Neu5Ac-aOH resulted in bound conformations near the predicted Asp-box. A local docking experiment of Neu5Ac-αOH was set up with a box size of 30 × 30 × 30 Å centered around the oxygen carbonyl atom at Thr-207 with 25 docking runs. Results from this local docking experiment revealed two clusters with bound Neu5Ac-αOH

(see Figure 2) identified as the main and secondary Neu5Ac binding sites. Two more complex Neu5Ac-containing glycans (α2-6-SLN-Ac and α2-3-SLN-Ac) were docked into the identified main Neu5Ac binding site using the same procedures as described above.

SPR analysis of the binding of *Pf*CyRPA to membranes of sialidase treated erythrocytes and of CRISPR/Cas9 knockouts

The immortalized erythroid human cell line BF was generated as described previously.[46–48] In short, $CD34^+$ bone marrow hematopoietic stem cells were transduced with the lentiviral vector CSIV-TRE-HPV16-E6/E7-UbC-KT and maintained under doxycycline treatment until stable cell growth was observed. BF cells were cultured in IMDM (Biochrome) supplemented with L-Glutamine (200mM, Sigma), Holo-transferrin (15 mg/ml, BBI solutions), Insulin (1 mg/ml, Sigma), Heparin (1 mg/ml, Fisher Scientific), 5% Octaplasm (Octapharma), animal component free stem cell factor (50 ng/ml, STEMCELL), animal component free EPO (3IU/ml, STEMCELL) and doxycycline (1 mg/ml, Sigma). To create CD44 and basigin knockout cell lines, 24pmol of each sgRNA (Integrated DNA Technologies) was pooled and allowed to complex with 237.9pmol Hi-Fi Cas9 (Integrated DNA Technologies) for 15 min. After complexation, the RNPs were added to the pelleted cells ($5x10^5$), mixed with human T cell nucleofection buffer (Lonza) and immediately transfected using the Amaxa Nucleofector 2b U-014 nucleofection program. The following sgRNAs were used: CD44 sgRNA-1 CCGATCTGCGCCAGGCTCAG,[49] sgRNA-2 CGTGGAATACACCTGCAAAG,[50] basigin sgRNA-1 CCATGATTCCTATTCCTCGC,[50] sgRNA-2 TTCACTACCGTAGAAG ACCT.[51]

Approximately one week after transfection, cells were single cell sorted and expanded clonal cell populations were screened for the absence of CD44 and/or basigin surface expression (Figure S1). 5 x 10^5 cells were resuspended in 100 μL PBS with 0.5% BSA and 2 mM EDTA and

were stained with REAfinity CD44-APC 1:50 (Miltenyi Biotec Cat# 130-113-900, RRID:AB_2726391) and REAfinity CD147-VioBlue 1:10 (Miltenyi Biotec Cat# 130-104-537, RRID:AB_2655192) for 10 min at 4°C. Cells were washed with PBS with 0.5% BSA and 2 mM EDTA and kept at 4°C prior to analysis with Miltenyi Biotec MACSQuant Analyzer 10 and FlowJo software (RRID:SCR_008520).

To test for INDEL formation in the selected clones, genomic DNA was isolated and the regions up- and downstream of both sgRNA cut sites were amplified using the following primer pairs: basigin sgRNA1 (fwd 5′-CAGGCCCCACTCCCGTTTCCTA-3′, rev 5′-CCGAAAAGCAAGACGCCCACCT-3′), sgRNA2 (fwd 5′- TCTCTGGGCAGGAACATCGCCA-3′, rev 5′- CCTCACAAGGACGCCCCTC AGA-3′), CD44 sgRNA1 (5′-TCTTAAAACCTCTGCGGGCT-3′, rev 5′-AGTCCAGACAACGACTGTGC-3′), sgRNA2 (fwd 5′-ATGGTGCTT TGGAATGCTGGA, rev 5′-GGCCAAGACTCTAACAGCCA-3′). To detect INDEL formation, Sanger sequencing files from wild type and knockout clone PCRs were used for TIDE analysis (https://tide.nki.nl; RRID:SCR_023704).[54]

For the preparation of cell membranes, wild type and knockout cells were washed with PBS and pelleted by centrifuging at 1,500 x g for 5 min. DNA was digested by addition of 5 mg/mL DNase. The pellet was washed four times in cold 5 mM sodium phosphate buffer (pH 8) and the lysed cells were centrifuged at 20′000 x g for 20 min and resuspended in cold 5 mM sodium phosphate buffer. The final pellet was resuspended in PBS and snap frozen in liquid nitrogen.

SPR analyses were used to analyze the interaction of cell membranes with *Pf*CyRPA by immobilizing membranes onto the flow cells of Series S C1 sensor chips with a flow rate of 5uL per minute in pH 5.5 sodium acetate with a minimum immobilization level of 1000 RU using a Biacore T200 (Cytivia). For analysis of the wild-type membranes, samples were immobilized onto FC2 and FC4 while FC1 and FC3 were left as blanks. The membranes on both flow cells were treated with 1x Glycobuffer 1 (NEB) with (FC4) or without (FC2) α2-3,6,8,9 Neuraminidase A for 30 min. Removal of sialic acid was confirmed with MAA. Analysis of the mutant membranes was carried out between two chips with the analysis of wild-type (FC2) and basigin −/− + CD44−/− (FC4) membranes used in both analysis as controls with either basigin −/− or CD44−/− membranes on FC3. For all analysis, CyRPA was run at a maximum concentration of 1μM across 5x 1 in 5 dilutions in triplicate. Analysis was carried out using the Biacore T200 evaluation software package with all data analyzed double background subtracted (empty flow cell and buffer control subtracted), with curve data copied to Microsoft Excel for reproduction. SPR sensorgrams are shown in Figure S8.

Immunofluorescence microscopy

Thin blood smears from highly synchronised, high parasitaemia segmented schizont cultures of *P. falciparum* strain 3D7 were air dried, fixed with 4% formaldehyde in PBS for 20 min, permeabilised with 0.1% Triton X-100 in PBS for 10 min and blocked with 3% bovine serum albumin in PBS for 1 h. Immuno-staining with 100 μg/mL mouse anti-*Pf*CyRPA mAb C10, which does not interfere with the glycan-binding activity of *Pf*CyRPA (Figures S5A and S5B), or with biotinylated glycans (α2-6-SLN-Ac or multimeric Poly [N-(2-hydroxyethyl) acrylamide-co-N-acrylamide]-coupled α2-6-SLN-Ac or α2-6-SLN-Gc; GlycoNZ, Auckland, NZ) was carried out for 1 h. After washing, slides were incubated with anti-mouse IgG-Alexa568 antibodies and streptavidin-Alexa488 (ThermoFisherScientific) at 1:1000 for 1 h, washed, and mounted with ProLong Gold antifade reagent with 4′,6-diamidino-2-phenylindole (DAPI) to stain the parasite DNA. Images were taken on a Leica DM-500B fluorescence microscope using a 100x oil immersion lens and processed with ICY bio image analysis software (icy; RRID:SCR_010587).

For the 3D7/*Pf*CyRPA-E148A-3xHA and 3D7/*Pf*CyRPA-recodonized-3xHA lines, thin blood smears from highly synchronous, segmented schizont cultures of Rapalog (250nM) treated and untreated 3D7/PfCyRPA-E148A-3xHA and 3D7/PfCyRPA-recodonized-3xHA were processed as described above and immunostaining was performed with primary antibodies rat anti-HA (Roche Cat# 11867423001, RRID:AB_390918, 1:500) and mouse anti-*Pf*CyRPA C10, (100 mg/mL) and fluorescently labeled secondary antibodies (goat anti-mouse Alexa 594, 1:1000 (Thermo Fisher Scientific Cat# A-11005, RRID:AB_2534073) and goat anti-rat Alexa 488,

1:1000 (Thermo Fisher Scientific Cat# A48262, RRID:AB_2896330). DNA was counterstained with Hoechst 33342 (1 μg/ml). Slides were mounted with Vecta Shield antifade mounting medium (Biozol). Images were taken on a Leica DM6B fluorescence microscope using a 100× oil immersion objective and analyzed and processed with FIJI software (Version 2.1.0 for Mac OS X; RRID:SCR_002285).

Generation of transgenic *P. falciparum* lines

The *Pf*CyRPAmut parasite lines were generated by 2 consecutive Cas9-mediated genome edits of a *P. falciparum* 3D7 parasites line allowing the conditional expression of the DiCre recombinase upon Rapalog treatment.[31] The general CRISPR/Cas9 plasmids used were described previously.[58] For the first round of gene editing, first the repair DNA plasmids pD-loxPint-CyRPAmut-3xHA for the various *Pf*CyRPA mutants were cloned. For this a PCR fragment corresponding to the 5′homology region (481 bp, corresponding to *cyrpa* bases 2124–2564, primers mut_HB1_f, mut_HB1_r, from 3D7 gDNA), a PCR fragment containing a SERA2loxPintron element, 846 bp of recodonized *cyrpa* sequence (1718–2564) encoding the desired point mutations and a 3xHA tag (primers mut_loxP_f, mut_loxP_r, from plasmid DNA encoding the *Pf*CyRPA mutant variants ordered as synthetic genes (Table S5) and a PCR fragment corresponding to the 3′homology region (444 bp, corresponding to the *cyrpa* 3′-UTR, primers mut_HB2_f, mut_HB2_r, from 3D7 gDNA) were assembled with an AmpOri PCR product using Gibson assembly as described earlier (Filarsky et al., 2018). In addition, the guide RNA target sequence 5′-AGACAAAAGGGGTTACTGCA-3′ was cloned into pY-gC using the BsaI restriction sites to generate pY-gC-loxPint-CyRPAmut-3xHA for Cas9 targeting of the *cyrpa* locus and selection via DSM1 as described earlier.[58] For the second round of gene editing, the repair DNA plasmid pD-CyRPA-loxPint-1 was cloned. For this a PCR fragment corresponding to the 5′homology region (506 bp, corresponding to *cyrpa* bases -231 – 243, primers loxPint1_HB1_f, loxPint1_HB1_r, from 3D7 gDNA), a PCR fragment containing a SERA2loxPintron element (128 bp, primers loxPint1_f, loxPint1_r, from pD-loxPint-CyRPAmut-3xHA) and a PCR fragment corresponding to the 3′homology region (400 bp, corresponding to the *cyrpa* bases 1617–1990, primers loxPint1_HB2_f, loxPint1_HB2_r, from 3D7 gDNA) were again assembled with an AmpOri PCR product using Gibson assembly as described above. In addition, the guide RNA target sequence 5′- CTTCTTTTGAACATATATAT-3’ was cloned into pH-gC using the BsaI restriction sites to generate pH-gC-CyRPA-loxPint-1 for Cas9 targeting of the *cyrpa* locus and selection via WR99210 as described earlier.[58] Synchronous ring stage parasite cultures were transfected with pD-loxPint-CyRPAmut-3xHA and pY-gC-loxPint-CyRPAmut-3xHA as described earlier. After reappearance of parasites, successful gene editing was verified with PCR on genomic DNA and parasites were cloned out as described previously.[59] Clones were then tested using PCR on genomic DNA again and positive clones were subjected to a second round of transfections with pD-CyRPA-loxPint-1 and pH-gC-CyRPA-loxPint-1 and treated as described above.

P. falciparum blood-stage culture

Parasites were cultured essentially as described previously.[60] The culture medium was supplemented with 0.5% AlbuMAX (Life Technologies) as a substitute for human serum.[61] Cultures were synchronized by sorbitol treatment.[62] Erythrocytes for passage were obtained from the Swiss Red Cross (Switzerland).

For the 3D7/*Pf*CyRPAmut lines parasite blood stages were cultured in human B^+ erythrocytes (Blutspendedienst UKE Hamburg, Germany) at a haematocrit of 5% in RPMI-1640 medium supplemented with 0.5% AlbuMAX II (Life Technologies), 25 mM HEPES, 0.36 mM hypoxanthine, 25.7 mM $NaHCO_3$ and 0.01% neomycin. The cultures were maintained in an atmosphere of 1% O_2, 5% CO_2 and 94% N_2 at 37°C.

Proliferation assay of 3D7/*Pf*CyRPAmut lines

To induce the excision of the *loxP* flanked sequences and consequent expression of the mutated *Pf*CyRPA protein variants, tightly synchronized ring stages cultures were divided into two dishes and one was treated with 250 nM Rapalog. In brief, late schizont parasites were isolated by Percoll (GE Healthcare) enrichment and allowed to reinvade into fresh RBCs for 3 to 4 h at 37°C under first shaking and then static conditions. The remaining schizonts were eliminated by sorbitol lysis. 24 h later at trophozoite stage the parasitemia of treated and untreated cultures were adjusted to 0.1% with a haematocrit of 5% by flow cytometry.

To investigate the effect of *Pf*CyRPAmut expression on parasite proliferation the treated and untreated parasites were monitored over 3 growth cycles. Medium was changed every day and the parasitemia was determined every 48 h at trophozoite stage. All cultures were diluted 1:10 within the second cycle.

For growth quantification, the parasites were stained with SYBR green dye (0.25x dilution in DMSO; Sigma Aldrich) and DHE (0.5 ng/μL in DMSO; Sigma Aldrich) for 30 min at room temperature. The samples were then analyzed in a Novocyte 1000 (ACEA Bioscience) flow cytometer. The RBCs were gated based on forward and side scatter parameters, and for 100,000 events SYBR green positive cells were identified and counted as infected cells.

Western blot analysis of 3D7/*Pf*CyRPAmut parasites

For the preparation of protein samples, synchronous ring stage cultures were split into Rapalog (250nM) treated and untreated control. After incubation of cultures at 37°C to late schizont stage Compound 2 (1 μM) was added to prevent egress and allow full maturation of all parasites. Parasites were lysed in 0.06% Saponin/PBS on ice for 15 min, sedimented at 2000 g and the pellet was washed in PBS until supernatant was clear. For protein extraction the pellets were incubated with 3x vol RIPA-Buffer (1% v/v NP40; 0.25%

w/v DOC; 10% v/v Glycerol; 2 mM EDTA; 137 mM NaCl; 20 mM Tris-HCl (pH 8) and 1x protease inhibitor) on ice for 15 min. Samples were then centrifuged at 20,000 g for 10 min at 4°C. 5x reducing SDS loading dye (416 mM Tris; 300 mM Tris-HCl (pH 6.8) 59.6 mM DTT; 60% v/v Glycerol and Bromphenol blue) was added to the supernatants and the samples were boiled for 5 min at 95°C. The protein lysates were separated on 10% SDS- polyacrylamide gels at 100 V for 30 min and another 90 min at 120 V and transferred onto a nitrocellulose membrane (LI-COR Bioscience) at 90 V for 60 min in a wet blot. The membranes were blocked in 5% w/v skim milk in TBS (150 mM NaCl; 10 mM Tris) for 1 h at room temperature. Primary (rat anti-HA (Roche Cat# ROAHAHA, RRID:AB_2687407) 1:1000, rabbit anti-BiP (1:2000; Struck)) and secondary IRDye 800CW goat anti-rat (LI-COR Biosciences Cat# 925–32219, RRID:AB_2721932 1:10,000) or IRDye 680RD goat anti-rabbit (LI-COR Biosciences Cat# 925–68071, RRID:AB_2721181 1:10,000) antibodies were diluted in 2.5% w/v skim milk and 0.05% v/v Tween20 in TBS (TBS-T). Primary antibodies were incubated o. n. at 4°C and blots washed 3 times in TBS-T before addition of the secondary antibody. After incubation at room temperature for 1 h the membranes were washed 3 times in TBS-T and once in TBS before being visualized on the Odyssey Fc Imaging System (LI-COR Biosciences) and analyzed with Image Studio Imaging Software (LI-COR Biosciences).

SPR drug screening of *Pf*CyRPA

SPR screening was performed as previously described[39] using the same capture method for *Pf*CyRPA as described above, with the following modifications: A combination of two libraries (Microsource-CPOZ: 2400 compounds; and ML Drug: 741 compounds) comprising drugs, dyes and other therapeutic molecules, were purchased from Compounds Australia and were screened at 1 μM with cocktails of eight compounds. Rescreening of positive cocktails as individual compounds was then carried out at 1 μM to determine the individual positive compounds. Post-screen, kinetic analysis was performed to determine the affinity of binding (equilibrium dissociation constant; KD) of compounds identified at 1 μM. The modification of this process reduces the number of SPR runs to determine useful binding compounds from a minimum of 10 SPR runs (~312 h of SPR time) to a minimum of 3 SPR runs (~60 h of SPR time). Competition assays (ABA – injection method according to the manufacturer's instructions; Cytiva S200) were performed between the identified compounds in competition with the CyRPA glycan target and the C12 antibody.

SPR competition assays of *Pf*CyRPA with antibodies and small molecules

SPR competition analysis was performed using a ForteBio Pioneer SPR system with CyRPA immobilized onto flow cell 1 of $COOH_5$ at 5 μL/min for 10 min in sodium acetate pH 4.0 at 25°C. OneStep and NextStep analyses were performed as previously described.[63] Binding to α2-6SLN-Ac (maximum of 10 μM) was competed with the drugs identified in drug screening (maximum of 10 μM) and previously published antibodies[5,10,11] (maximum of 10 μg/mL).

P. falciparum blood-stage culture

Parasites were cultured essentially as described previously.[60] The culture medium was supplemented with 0.5% AlbuMAX (Life Technologies) as a substitute for human serum.[61] Cultures were synchronized by sorbitol treatment.[62] Erythrocytes for passages were obtained from the Swiss Red Cross (Switzerland).

In vitro growth inhibition assay (GIA)

The EC_{50} values for repurposed drugs were determined *in vitro* by measuring incorporation of the nucleic acid precursor [^{3}H]-hypoxanthine. Infected erythrocytes were exposed to increasing concentrations of compounds in culture plates. After 48 h of incubation, 0.5 μCi [^{3}H]-hypoxanthine was added to each well. Cultures were incubated for a further 24 h before being harvested onto glass-fibre filters and washed with distilled water. The radioactivity was counted using a Betaplate liquid scintillation counter. The results were recorded as counts per minute per well at each compound concentration and were expressed as a percentage of the untreated controls. For each compound, a four-parameter sigmoidal dose-response curve was fitted to the relationship between the $\log_{10}$ (compound concentration) and % inhibition, and was then used to interpolate the EC_{50} values. Data were processed and analyzed using GraphPad Prism 7 (GraphPad Software, Inc., La Jolla, CA, USA).

Monoclonal antibodies (mAbs) specific for *Pf*CyRPA and *Pf*RH5

Generation of anti-*Pf*CyRPA[10,33] and anti-*Pf*RH5 mAbs[11] has been described elsewhere. Monoclonal antibodies were purified by affinity chromatography using protein A Sepharose (Cytiva, Marlborough, MA, USA). mAbs were grouped into epitope bins A–F[11] by determining the reactivity patterns with overlapping fragments of *Pf*CyRPA, as described previously.[5,10] The three mAbs that inhibit *Pf*CyRPA-*Pf*RH5 interaction (C05, C13 and SB3.9) belong to epitope bins D and E.

Cloning, expression, and purification of *Pf*RH5

A synthetic gene (GenScript) encoding the *Pf*RH5 residues E26-Q526 from *P. falciparum* strain 7G8, was codon optimized for expression in *Drosophila melanogaster* S2 insect cells. The coding sequence is flanked by a BamHI site and Kozak sequence at the 5′ end, and a NotI site at the 3′ end. The resulting expression vector pExpreS2.1-*Pf*RH5(E26-Q526) also encodes the *Drosophila* BiP signal sequence for secretion into the cultivation medium, and a C-terminal 8xHis-tag. Constructs were transfected into Schneider 2 (S2) cells using TRx5 ExpreS2 insect cell transfection reagent (ExpreS2ion Biotechnologies). A polyclonal cell line was selected over three weeks in EX-CELL 420 insect cell media with L-glutamine (Sigma) and 1.5 mg/mL Zeocin. After the selection process, stable cell lines

were expanded in EX-CELL 420 media. 72h after the final split, the cells were removed by filtration and the cell culture supernatant equilibrated to pH 7.4 and cOmplete Protease Inhibitor Cocktail (20 tablets per liter of cell culture supernatant; Roche Diagnostic). The 8xHis-tagged recombinant PfRH5 was purified by immobilized metal ion affinity chromatography (IMAC) on a cOmplete His-Tag Purification Column (5 mL volume; Roche Diagnostic). The eluate was concentrated by ultra-filtration (Amicon Ultra-15 Ultracel 30K, Millipore) and applied to Superdex 200 Increase 10/300 GL gel filtration column (GE-Healthcare) equilibrated with 50 mM Imidazole pH 7.0, 500 mM NaCl, 10% glycerol, cOmplete Protease Inhibitor (4 tablets/L). Homogeneity of *Pf*RH5 was assessed by reversed-phase chromatography (RP-HPLC) on a Poroshell 300SB-C8 5μm, 1 × 75 mm column using a H_2O + 0.01% TFA/Acetonitrile +0.08% TFA gradient, and was confirmed by LC/MS intact mass analysis.

*Pf*CyRPA-*Pf*RH5 mAb competition experiments

ELISA Maxisorp plates (Nunc) were coated with 50 μL of PBS per well containing 10 μg/mL of purified recombinant *Pf*CyRPA for 16 h at 4°C. Plates were then washed three times with PBST (PBS with 0.05% (v/v) Tween 20), and plates were blocked with 5% non-fat dry milk/PBS for 1 h at 21°C. After the plates were blotted dry, 100 μL of a mixture, containing 0.5 μg/mL of recombinant *Pf*RH5 and anti-*Pf*CyRPA mAbs (tested at 10, 5, 1 and 0.1 μg/mL) in 0.5% MPBST (0.5% non-fat dry milk/PBS supplemented with 0.05% (v/v) Tween 20), was added to each well and incubated for 1 h at 21°C. Following washing, 50 μL of 10 μg/mL biotinylated anti-*Pf*RH5 mAb BS1.2 in 0.5% MPBST were added to each well and incubated for 1 h at 21°C. Binding of the biotinylated mAbs was detected by using HRPO-conjugated streptavidin (Sigma-Aldrich) as detecting agent (diluted at 0.5 μg/mL in 0.5% MPBST and incubated for 1 h at 21°C), and tetramethylbenzidine substrate (KPL) for development. The color reaction was stopped after 15 min of incubation (21°C in the darkness) by adding 50 μL of 0.5 M H_2SO_4 and the absorbance at 450 nm was measured using a Sunrise Absorbance Reader (Tecan).

QUANTIFICATION AND STATISTICAL ANALYSIS

For Array analysis Microsoft Excel (RRID:SCR_016137) was utilised for statistical analysis (Student's unpaired t test of fluorescence of the background spots vs. fluorescence of the glycan printed spots). Results were obtained from three arrays and a total of 12 data points per glycan. Data is presented as average fold above background (plus 3x standard deviation of the background).

All other statistical analyses were performed using GraphPad Prism 7 (GraphPad Software, Inc., La Jolla, CA, USA). Number of samples is presented in each legend and all data is reported plus/minus 1x standard deviation.